ENVIRONMENTAL AND ECONOMIC RESEARCH AND DEVELOPMENT PROGRAM

Contributions of Fossil Fuel-fired Electric Power Generation to PM2.5 Concentrations in Wisconsin

Final Report
December 2012

PREPARED BY:

PROJECT PI:

PROF. JAMES J. SCHAUER, UNIVERSITY OF WISCONSIN-MADISON

PROJECT CO-PIs:

PROF. BEN DE FOY, SAINT LOUIS UNIVERSITY;
PROF. WILLIAM CHRISTENSEN, BINGHAM YOUNG UNIVERSITY;

PROJECT CONTRIBUTORS:

PROF. DEBORAH GROSS, CARLETON COLLEGE;
DR. JONGBAE HEO, UNIVERSITY OF WISCONSIN-MADISON;
ALISON M. SMYTH, CARLETON COLLEGE;
SAMANTHA L. THOMPSON, CARLETON COLLEGE;
JEROME McGINNIS, UNIVERSITY OF WISCONSIN-MADISON;
MIKE OLSON, UNIVERSITY OF WISCONSIN-MADISON;
NICK SAGAR, UNIVERSITY OF WISCONSIN-MADISON;

focus on energy℠
Partnering with Wisconsin utilities

This report was funded through the Environmental and Economic Research and Development Program of Wisconsin's Focus on Energy.

List of Figures

List of Tables

List of Abbreviations

ANOVA = ANalysis Of VAriance

AQS = Air Quality System

ATOFMS = Aerosol Time Of Flight Mass Spectrometer

BC = Black Carbon

CAMx = Comprehensive Air quality Model with eXtensions

CFA = Concentrations Field Analysis

EC = Elemental Carbon

EDAS = Eta Data Assimilation System

FIPS = Federal Information Processing Standard

HYSPLIT = Hybrid Single-Particle Lagrangian Integrated Trajectory

IC = Ion Chromatography

KENW = Climatic Data for Kenosha

KFLD = Climatic Data for Fond du Lac

KMKE = Climatic Data for Milwaukee, General Mitchell International Airport

KMSN = Climatic Data for Madison/Dane County Air port

KRAC = Climatic Data for Racine

LADCO = Lake Michigan Air Directors COnsortium

MANOVA = Multivariate ANalysis Of VAriance

MCMC = Markov Chain Monte Carlo

MDL = Method Detection Limit

NAAQS = National Ambient Air Quality Standard

NEI = National Emission Inventory

OC = Organic Carbon

PCA = Principal Component Analysis

PM2.5 = Particulate matter less than 2.5 micrometer in diameter

PMF = Positive Matrix Factorization

PSCF = Potential Source Contribution Function

QAQC = Quality Assurance/Quality Control

SER = South East Regional Headquarters

SOA = Secondary Organic Aerosol

STN = Speciation Trends Network

WDNR = Wisconsin Department of Natural Resources

WRF = Weather Research and Forecasting Model

XRF = X-Ray Fluorescence

Executive Summary

The goal of the project was to incorporate state-of-the-art receptor and inverse transport models to quantify the contribution of fossil fuel-fired electric power generation to PM2.5 concentrations in Wisconsin. The project integrated four main components to achieve the overall project goal: 1) analysis of trends in the concentrations and components of historical PM2.5 measurements in Southeastern Wisconsin, 2) application of a multi-variant receptor model to existing PM2.5 monitoring data collected as part of the EPA Speciation Trends Network in Milwaukee (Site 550790026), Waukesha (Site 551330027), and Mayville (Site 550270007), 3) collection of targeted high time resolution PM2.5 chemical composition data used to understand the climatology that lead to speciated PM2.5 concentrations at rural and urban locations in Wisconsin, and 3) employ an inverse transport model and Concentrations Field Analysis (CFA) to identify the spatial distribution, including point, mobile, and area sources of speciated PM2.5 concentrations in Wisconsin.

A key conclusion of the project was that annual average concentrations of PM2.5 sulfate ion and PM2.5 nitrate ion at the Milwaukee and Waukesha sites were not statistically different from the concentrations observed in Mayville providing strong evidence that these PM2.5 components are largely transported into Southeast Wisconsin and are not greatly impacted by local emissions. The urban excess of PM2.5 for these sites is dominated by carbonaceous aerosols, which were found to be largely associated with local emissions of mobile sources and biomass burning. Given that ammonium sulfate and ammonium nitrate contribute approximately 50-60 percent of the annual average PM2.5 concentrations in Southeast Wisconsin and organic carbonaceous aerosol makes up another 25-35 percent, PM2.5 mitigation strategies need to address these PM2.5 components. Analysis of meteorological data demonstrates that days with high PM2.5 sulfate ion concentrations are associated with long range transport from the Ohio Valley, and high PM2.5 nitrate ions are associated with long range transport from the Ohio Valley and other regions of the Midwestern United States. The results demonstrate that although fossil fuel fired power generation is impacting the PM2.5 concentration and non-attainment periods; these impacting emissions are not local to Southeast Wisconsin and are emissions in other regions of the country. Reductions of PM2.5 mass concentrations in Southeast Wisconsin should be

directed at carbonaceous aerosol associated with mobile sources, biomass burning and emissions from stationary power generation in the Ohio Valley.

Local point sources in Southeastern Wisconsin, including stationary power generation, does impact local concentrations of trace components of particulate matter including trace metals, black carbon, and bromine. Although these are not major contributors to PM2.5 concentrations and reduction in emissions of these components are not likely to provide a significant impact in reducing PM2.5 concentrations, there may be potential air quality and human health benefits from reducing these emissions.

The details of the study are outlined in this report and are summarized in four manuscripts that have either been accepted for publication or will be submitted for consideration for publication in the near future. These publications are listed below.

Project Publications

1) J. E. McGinnis, J. Heo, M. R. Olson, A. P. Rutter, and J. J. Schauer. Understanding the Sources and Composition of the Urban Excess of Fine Particulate Matter. In preparation for submission for publication.

2) J. Heo, J. E. McGinnis, B. de Foy, and J. J. Schauer. Identification of Potential Source Areas for Elevated PM2.5, Nitrate and Sulfate Concentrations in the Southern-Wisconsin. In review for publication.

3) A. M. Smyth, S. L. Thompson, B. de Foy, M. R. Olson, N. Sager, J. J. Schauer, and Deborah S. Gross. Sources of Metals and Bromine-Containing Particles in Milwaukee. In review for publication.

3) B. de Foy, A. M. Smyth, S. L. Thompson, D. S. Gross, M. R. Olson, N. Sager, and J. J. Schauer. 2012. Sources of Nickel, Vanadium and Black Carbon in Aerosols in Milwaukee .*Atmospheric Environment.* 59, 294-301.

Introduction

Ambient fine particulate matter (PM2.5) is a major air quality concern because of its adverse health effects [*Pope et al., 2009*]. To mitigate the health effects of $PM_{2.5}$, the United States Environmental Protection Agency (US EPA) promulgated a national ambient air quality standard (NAAQS) for $PM_{2.5}$ in 1997. Due to growing evidence of substantive health effects at low-to-moderate $PM_{2.5}$ concentrations that are common to many communities throughout the US [*Pope and Dockery, 2006*], the US EPA lowered the 24-hour $PM_{2.5}$ standard from 65 $\mu g/m^3$ to 35 $\mu g/m^3$ in September 2006. The revised standard focuses on the extreme events or episodes, in which daily mass concentrations are substantially higher than the annual average. Finding the conditions that lead to high $PM_{2.5}$ episodes has been challenging to states, tribal lands and local governments and has made compliance with the 24-hour average standard difficult.

The elevated $PM_{2.5}$ episodes have been consistently observed in northern cities in the Midwest. In August 2011, the US EPA designated the southern Wisconsin area, including Milwaukee, Racine, and Waukesha Counties, as being in non-attainment of the 2006 $PM_{2.5}$ NAAQS. To provide a better understanding of these episodes and to make a strategic plan for compliance with the standard, a number of studies have been conducted and have concluded that specific meteorological conditions lead to high $PM_{2.5}$ episodes in the region. For example, the report of the Conceptual Model of $PM_{2.5}$ Episodes in the Midwest [*LADCO, 2009*] stated that the $PM_{2.5}$ episodes occur across broad areas in the upper Midwest and are mostly driven by stagnant air conditions with high pressure, slow southerly wind speeds and high relative humidity. Katzman et al. [*2010*] reported elevated $PM_{2.5}$ episodes occur more often in winter than in summer in northern cities in the Midwest, and wintertime episodes are strongly enhanced by nitrate under a stagnant weather pattern. Furthermore, Beak et al. [*2010*] showed wintertime episodes in the region are marked by inversions with a shallow, stable planetary boundary layer, warm, moist air and low wind speeds.

This project addresses the impacts of existing fossil fuel-fired electric power generation on PM2.5 levels in Wisconsin. The overall goal of the project was to determine the relationship between sulfur dioxide emissions and nitrogen oxide emissions from existing fossil fuel-fired electric power generation facilities within the State of Wisconsin, and to distinguish the impact of emissions from outside the State of Wisconsin on PM2.5 concentrations in PM2.5 non-

attainment counties in Wisconsin. The project addresses emissions impacts on the annual and 24-hour PM2.5 Federal National Ambient Air Quality Standard (NAAQS). Prior work by the project team has demonstrated winter time exceedances of the PM2.5 standard are largely associated with high ammonium nitrate concentrations, while in contrast; summer time exceedances are largely associated with high sulfate and high secondary organic aerosol (SOA) concentrations. Although fossil fuel fired electric power generation facilities represent significant emissions of sulfur dioxide, nitrogen oxides, and precursors for photochemical smog linked to SOA production, there are also other significant sources of PM2.5 precursors. For this reason, there is a great need to accurately determine the relative contributions of the precursor emissions from specific emissions categories and facilities on PM2.5 concentrations using advanced source apportionment methods. The use of emissions inventory estimates of PM2.5 precursors in traditional atmospheric transport models is insufficient for good air quality management. More advanced methods are needed to provide accurate apportionment results.

Methods

Analysis of Speciation Trends Network Data

The Speciation Trends Network (STN) reported every three day PM2.5 measurement data for Milwaukee and Mayville, and every six day concentrations for Waukesha via the Air Quality System (AQS). The concentration of $PM_{2.5}$ as well as the concentrations of the chemical species present in $PM_{2.5}$ were included in the STN data and include elemental carbon (EC), organic carbon (OC), nitrate, sulfate, ammonium, chloride, and potassium ion along with 48 elements. X-Ray Fluorescence (XRF) Spectrometry was used on Teflon filters to determine the concentrations of the 48 elements. Ion Chromatography (IC) was used on nylon filters for determining the concentrations of sulfate, nitrate, ammonium, sodium and potassium. The data in the STN database was not blank subtracted, but the STN contained concentrations from blanks that were analyzed as part of the measurements. The average of the field blanks from the Milwaukee, Mayville, and Waukesha sites was determined for each chemical species. These average field blank concentrations were used to perform the blank subtraction for each species.
Quality assurance/quality control (QAQC) was performed on the data to remove any invalid data. Dates were flagged on the raw STN data file when the monitoring device was running incorrectly. This included machine malfunctions, power failures, invalid flow rates and other

issues. Flagged data was reviewed and used to remove invalid data from the data set. Blank subtraction was performed using the average and standard deviation of the blanks from the AQS data. The method detection limit (MDL) was calculated for each element using three times the standard deviation of the blanks. The number of data points above the MDLs were identified for each element at each location and percentages greater than 10% above the MDLs were used to determine what compounds and elements were incorporated into the data analysis. The PM2.5 data included in the analysis were EC, OC, nitrate, sulfate, ammonium, chloride and potassium ion along with 24 elements. Sodium and sulfur XRF data and potassium from the IC analysis were removed to avoid duplication of chemical species. A total of 28 chemical species were used in the data analysis. Outliers were determined using box plots and scatter plots.

Positive Matrix Factorization

Using the STN data, source apportionment was determined using Positive Matrix Factorization (PMF). PMF [*Paatero and Tapper*, 1994] is an advanced factor analysis technique based on a weighted least-squares fit and error estimates of the measured data. In this study, measurement uncertainties provided by the STN database were used for the error estimates. Data below method detection limits (MDL) were assigned values equal to half the corresponding MDL, and error estimates were assigned values 5/6 of each species' MDL [*Polissar et al.*, 1998]. XRF sulfur and IC sulfate were in good agreement, however, the XRF sulfur data was removed to avoid double counting of mass concentrations in the model. XRF sodium and XRF potassium were included in the analysis because of higher analytical precision than IC sodium and potassium ion. Data from firework event days (July 4 and 5) were excluded to avoid distortion of specific factor contributions through abnormally high emissions of several elements. A total of 789, 781, and 395 samples were included for Milwaukee, Mayville, and Waukesha sites, respectively, which spanned data collected from 2002 through 2008.

The PMF model was run with a different number of sources to determine the best solution and different pseudorandom numbers were examined for the iterative fitting process. The robust mode and FPEAK matrix were used to reduce the effects of extreme values and reduce the rotational ambiguity respectively. Rotational ambiguity is a major problem in the application of multivariate analysis to environmental data. In the PMF model, a user-specified parameter called FPEAK is contained to control factor-rotational ambiguity of the solution like the varimax

method of traditional factor analysis. A FPEAK parameter was applied using different values from -1.0 to 1.0 in this study. To obtain the quantitative factor contributions, the PMF factors were normalized by scaling constants which were calculated from multiple linear regressions relating $PM_{2.5}$ mass concentration to the factor contributions from the PMF. In order to select an optimal number of factors, the mathematical PMF diagnostics (model error, Q, rotational ambiguity, and rotmat) and interpretable testing of the plausibility of the PMF solution were examined. Finally seven-source models with FPEAK = -0.4, nine-source models with FPEAK = -0.4, and nine-source models with FPEAK = 0.0 provided the physically realistic profiles for Mayville, Waukesha, and Milwaukee sites, respectively.

Potential Source Contribution Function (PSCF) Analysis

There is strong evidence that long-range transported air pollutants can have an effect of increasing gases and particles concentrations in urban and rural atmospheric environments. In some parts of the Midwestern US, sulfate and nitrate concentrations in fine particles have been influenced by the air masses and paths that originate in polluted remote areas and thus bring additional pollutants to receptor sites [*Kim and Hopke*, 2004; *Lee and Hopke*, 2006; *Zhao and Hopke*, 2006]. Consequently, several counties in this region may fail to comply with the current ambient air quality standards for PM2.5 due to uncontrollable excess of PM2.5 mass from outside non-attainment area. Therefore, it is necessary to investigate the long-range transport trends of pollutants, to estimate their contributions and to trace where the origins and paths of air masses lead to increasing pollutants levels at receptor sites using appropriate methods. Statistical methods for combining the measurements of gaseous and particle air pollutants and backward trajectories of air parcels calculated for corresponding times have been applied effectively in many atmospheric studies to investigate the likely source regions and preferred transport directions that can contribute to the elevated air pollutants at receptor sites [*Ashbaugh et al.*, 1985; *Kim and Hopke*, 2004; *Zhao and Hopke*, 2006]. The Potential Source Contribution Function (PSCF) which is a single trajectory based method [*Ashbaugh et al.*, 1985] has been seen as a simple and valuable tool for identifying likely source locations of long-range transported air pollutants.

The PSCF model was applied to identify the source region contributing to the elevated PM2.5 mass and sulfate and nitrate concentrations in southern Wisconsin. The back trajectories were

calculated using the Hybrid Single-Particle Lagrangian Integrated Trajectory model (HYSPLIT 4.9 version) using the Eta Data Assimilation System (EDAS) 80 km and the EDAS 40 km gridded meteorological data from 2002 through 2010 [*Draxler and Rolph, 2012*]. Five-day backward trajectories arriving at heights of 500 m above ground level at the receptor site at every hour intervals were computed using a vertical velocity model for every 24-hour integrated samples. The measured concentration values were assigned to the grid cells of 1º × 1º geographical coordinates (latitude and longitude) along the corresponding back trajectories. The likely source locations representing high PSCF values were calculated by the equation: $PSCF_{ij}=m_{ij}/n_{ij}$, where n_{ij} is the total number of end points that pass through the grid cell (i, j), and m_{ij} is the number of end points associated with samples that exceed the threshold criterion values in the same grid cell. In this study, the upper 25% of PM2.5 mass, sulfate and nitrate concentrations were used as the threshold criterion. Other threshold criteria, including the lower 25% of each of the observed data and PM2.5 mass greater 30 μg/m^3, were also investigated as a sensitivity analysis. The small number of total trajectories can result in high PSCF values with high uncertainties, therefore, an arbitrary weight function [*Polissar et al.*, 2001] was applied to reduce this effect in which the total number of end points was less than three times the average number of end points.

Summer Intensive Data Collection

The Carleton College Aerosol-Time-of-Flight Mass Spectrometer (ATOFMS) instrument sampled aerosol particles during the summer of 2010 in Milwaukee, WI. Analysis of the data, supported by the National Science Foundation, followed two main directions:

1. Identification of metal ions observed in particles, correlation of observations of these ions with meteorological patterns, and inferences about their sources. Certain metals known to be indicative of specific sources were the primary focus.

a. Molybdenum, cadmium, antimony, and selenium from power plants

b. Vanadium and nickel from heavy oil combustion (ships)

2. Investigation of bromine in particles, correlation of observations of this species with meteorological patterns, and determination of potential sources locations.

Continuous semi-real time data was collected at the Wisconsin Department of Natural Resources (WDNR) South East Regional Headquarters (SER) STN site (43° 3'39.20"N, 87°54'49.22"W) during July and August 2010. The inlet for the sample manifold is located on top of the SER building, approximately 10 meters above ground surface. A one inch stainless steel sample line transitions into a glass manifold from which the samples were collected; a medium volume pump continually evacuates excess air flow from the air inlet system. Monitoring equipment included the following: API SO2 Monitor (Teledyne, San Diego, CA) – collected sulfur dioxide concentrations every five minutes; URG Ambient Ion Monitor (AIM, URG, Chapel Hill, NC) – collected sulfate, nitrate and ammonium concentrations every hour; and Magee Aethalometer AE31 (Magee Scientific, Berkley, CA) – collected seven wavelength optical absorptions every five minutes, the instrument's internal algorithm was applied to quantify black carbon (BC) concentrations at 880 nm wavelength, no corrections were applied. All results were summarized into hourly averages for data analysis. Instruments were operated as per the manufactures recommendations and QA/QC spikes and blanks were performed weekly.

Winter Intensive and Summer Intensive Modeling

Mesoscale meteorological simulations were performed using the Weather Research and Forecasting Model (WRF) version 3.3.1 [*Skamarock et al. 2005*]. The boundary and initial conditions were obtained from the North American Regional Reanalysis which has a resolution of 32 km. WRF was run with two-way nesting on 3 domains of 27, 9 and 3 km resolution with 41 vertical levels. The Yonsei University (YSU) boundary layer scheme was used along with the the Kain-Fritsch convective parametrization, the NOAH land surface scheme, the WSM 3-class simple ice microphysics scheme, the Goddard shortwave scheme and the RRTM longwave scheme. Individual simulations each lasting 162 hours were performed: the first 42 hours were considered spin-up time, and the remaining 5 days were used for analysis.

Back-trajectories were calculated every hour for each campaign at the measurement sites using the FLEXPART model [*Stohl et al.*, 2005] and WRF wind field information. These were used for diagnostic analysis of individual pollution episodes. In addition, Concentration Field Analysis was used to identify possible source regions [*De Foy et al.*, 2007]. Sensitivity tests were performed with alternative configurations of the WRF models which showed the results were robust to individual choices in modeling options.

Supplemental data was obtained from the Lake Michigan Air Directors COnsortium (LADCO), which was obtained from the EPA funded Winter Nitrate Study. The data collected from this study was obtained under QA/QC review from the US EPA and is publicly available. The Winter Nitrate Study includes real-time measurements of gas-phase and particle-phase nitrogen compounds, which are components of, or precursors to PM2.5.

Synoptic analysis and classification

The meteorological analysis used integrated wind surface hourly data from the National Climatic Data Center. For clustering, 5 stations in southeastern Wisconsin with the most complete datasets were used: KMKE (Milwaukee / General Mitchell International Airport), KRAC (Racine), KENW (Kenosha), KFLD (Fond du Lac) and KMSN (Madison / Dane County Airport). Data were averaged to daily values for the clustering in order to coincide with the STN data sampling. Missing data at individual sites were interpolated from neighboring sites in order to minimize the number of days with missing clusters. Based on an examination of the distance within clusters, 8 clusters were selected for the analysis. K-means clustering was used with a random seed to initialize the clusters. Analysis of 20 separate runs of the clustering algorithm showed the results were not sensitive to the random seed.

Source Apportionment using Multiple Sites and Synoptic Regime Information

In this project we propose two extensions to existing work in Bayesian PSA:

1. Addressing pollution measurements from multiple sites in the same region and fitting common sources but allowing contribution levels to vary by site.

2. Exploring the relationship between synoptic regimes, or large-scale weather patterns and pollution contributions, and whether this additional information can be exploited to better estimate contributions.

A Bayesian model was proposed for the first extension and a post hoc statistical analysis on the estimated profiles, as well as a Bayesian model which may help include information about synoptic regimes in the estimation process was the second proposed extension. Bayesian inference was performed using MCMC code written in MATLAB to draw from the posterior distributions.

Multiple Locations

To estimate pollution source profiles and contributions when pollution measurements are available from several locations in the same region (i.e., close enough that the major pollution sources are expected to be the same) the following model was applied: Given data matrices Y1, Y2,…, Ym from the same region:

$$\begin{aligned}\mathbf{Y}_1 &= \mathbf{\Lambda}\mathbf{F}_1 + \mathbf{E}_1 \\ \mathbf{Y}_2 &= \mathbf{\Lambda}\mathbf{F}_2 + \mathbf{E}_2 \\ &\vdots \\ \mathbf{Y}_m &= \mathbf{\Lambda}\mathbf{F}_m + \mathbf{E}_m,\end{aligned}$$

where common profiles are estimated across all m sites but have separate contributions matrices. This model fits the assumption of source profile invariance, while making allowance for different amounts of pollution from each source that was present at each measurement station due to geography and possible station-specific effects, such as local air flow patterns.

The multiple sites model described above were successfully fitted using data from the Milwaukee, Waukesha, and Mayfield measurements stations. Because data was collected at different intervals at the different sites, only 343 observations were available in the collection period between 2002 and 2008 which equated to roughly one observation per week.

To evaluate the trade-off between using fewer data points from all three sites and using more frequent measurements from a single site, we fit a model to the 789 observations from the Milwaukee site, which has the most observations (one every three days). Both models used the same prior information on Λ, which is of primary interest, and the same non-distinguishing priors on the elements of F. On average, equal-tail 95% credible intervals for the elements of Λ from the model using data from all three sites were about 85% as wide as equivalent credible intervals from the model using data from the Milwaukee site. It is clear that drawing observations from multiple sites can increase model precision even when working with a small data set. If multiple sites with the same frequency of measurements were available, this would allow fitting a model and obtaining equivalent precision using data from a much shorter time span than if only data from one site were used, which would help mitigate the effects of violations of the assumption of profile invariance over time.

Synoptic Regimes

Because of the potentially large effect of weather patterns on air pollution, the relationship between the synoptic regimes identified by a meteorologist and the estimated source contributions were explored. As an initial investigation, a simple MANOVA using the synoptic regime classifications for each measurement period as an independent variable and the estimated contribution levels as responses was performed. The synoptic regimes may affect pollution measurements in several ways; the easiest to identify was source masking, in which particular synoptic regimes cause the pollution emitted by one or more sources not to reach the measurement stations. For example, particulate matter may be washed out of the air by a rain storm, or prevailing winds may shift it away from the measurement station. In these cases, though the source may still be emitting pollution, it will not be measured at typical levels. This type of effect should be easily identified by the MANOVA procedure if the model estimation is able to pick it up.

When synoptic regimes are related to weather patterns and show a masking effect, we considered another extension to the basic model which allows for the estimation of these masking effects. Namely, for each time period a classification is provided into one of the r synoptic regimes. For simplicity a single site was used for this analysis. We construct the $r \times t$ regime matrix R as a binary matrix where the (i, j) entry is 1 if time period j is classified into regime i and 0. Thus, 1 appears once in each column of R.

A $k \times r$ matrix M (masking matrix) is introduced into the model, which is also a binary matrix, but is estimated during the MCMC process. A value of 1 in the (i, j) entry of M indicates that the ith source is measured normally under the jth regime; a 0 indicates under the jth regime the source is masked.

The basic model is then given by

$$Y = \Lambda [F \circ (MR)] + E$$

where $\circ$ indicates the Hadamard product (element-wise multiplication). In effect, for each element of F this model determines whether the source in question was masked at the given time period, and if so, zeros out that location. This model may be estimated with standard MCMC techniques.

Results

Speciation Trends Network Data Analysis

Figure 1 represents the breakdown of the annual average $PM_{2.5}$ speciation for each study years at each location. In this figure the "Other Measured Elements" refers to reported elements and ions excluding the major constituents included in the plots. This figure shows similar trends for the constituents over the years at each location with the highest $PM_{2.5}$ concentration occurring in 2002 and 2005. There is a higher concentration of most constituents and total $PM_{2.5}$ at Milwaukee and Waukesha compared to Mayville and no significant change in the total $PM_{2.5}$ from 2002-08 at any location.

Urban excess was calculated by subtracting concentrations at the rural Mayville site from the urban sites. These values were then compared to the uncertainty of the calculated urban excess to determine if the values were statistically different from zero. Figure 2 shows the statistically significant excess in Milwaukee compared to Mayville, and Waukesha compared to Milwaukee. Figure 2a shows on average there is a statistically significant amount of excess elemental carbon ($.236 \pm .029$ µg/m^3), organic matter ($1.79 \pm .37$ µg/m^3), and crustal elements ($.064 \pm .038$ µg/m^3) in Milwaukee compared to Mayville. Figure 2b shows there is an excess in the amount of crustal elements ($.151 \pm .077$µg/m^3) in Waukesha compared to Milwaukee. The crustal elements included in this analysis are aluminum, calcium, lead, magnesium, titanium, silicon and potassium.

The urban element excess was expanded to highlight iron, silicon, calcium, zinc, and magnesium. From Figure 3 shows Waukesha has an excess of metals compared to Milwaukee and Milwaukee has an excess relative to Mayville. Figure 3a shows there is an excess of iron, silicon, calcium, and zinc in Milwaukee compared to Mayville. Figure 3b shows an excess of iron, silicon, calcium, zinc, and magnesium in Waukesha compared to Milwaukee. Waukesha has a significant excess of Magnesium compared to Milwaukee, however, no excess is seen comparing Milwaukee to Mayville. Overall, Waukesha has the largest excess relative to Milwaukee of select trace elements. The sum of the differences in these metals accounts for on

average only 5 percent of the urban excess in Milwaukee compared to Mayville, but accounts for 21% of the urban excess in Waukesha compared to Milwaukee.

Concentrations for all individual compounds and elements between two sites were compared to determine the correlations of major components across the sites. When comparing Milwaukee vs. Mayville, the slope was statistically greater than one for sulfate ion, ammonium ion, chloride ion, iron, manganese, sulfur, terbium and potassium ion. This indicates these compounds and elements are likely to have significant local sources in Milwaukee. The Milwaukee versus Waukesha comparison of the metals except sulfur and bromine have slopes significantly less than one, indicating these are most likely local sources from Waukesha.

Timescales for all three sites were reviewed and at least two sites showed statistically significant decreases in arsenic, lead and selenium from 2002-2008. Chloride ion and bromine were the only elements that showed a statistically significantly increase from 2002-2008 in at least two of the sites.

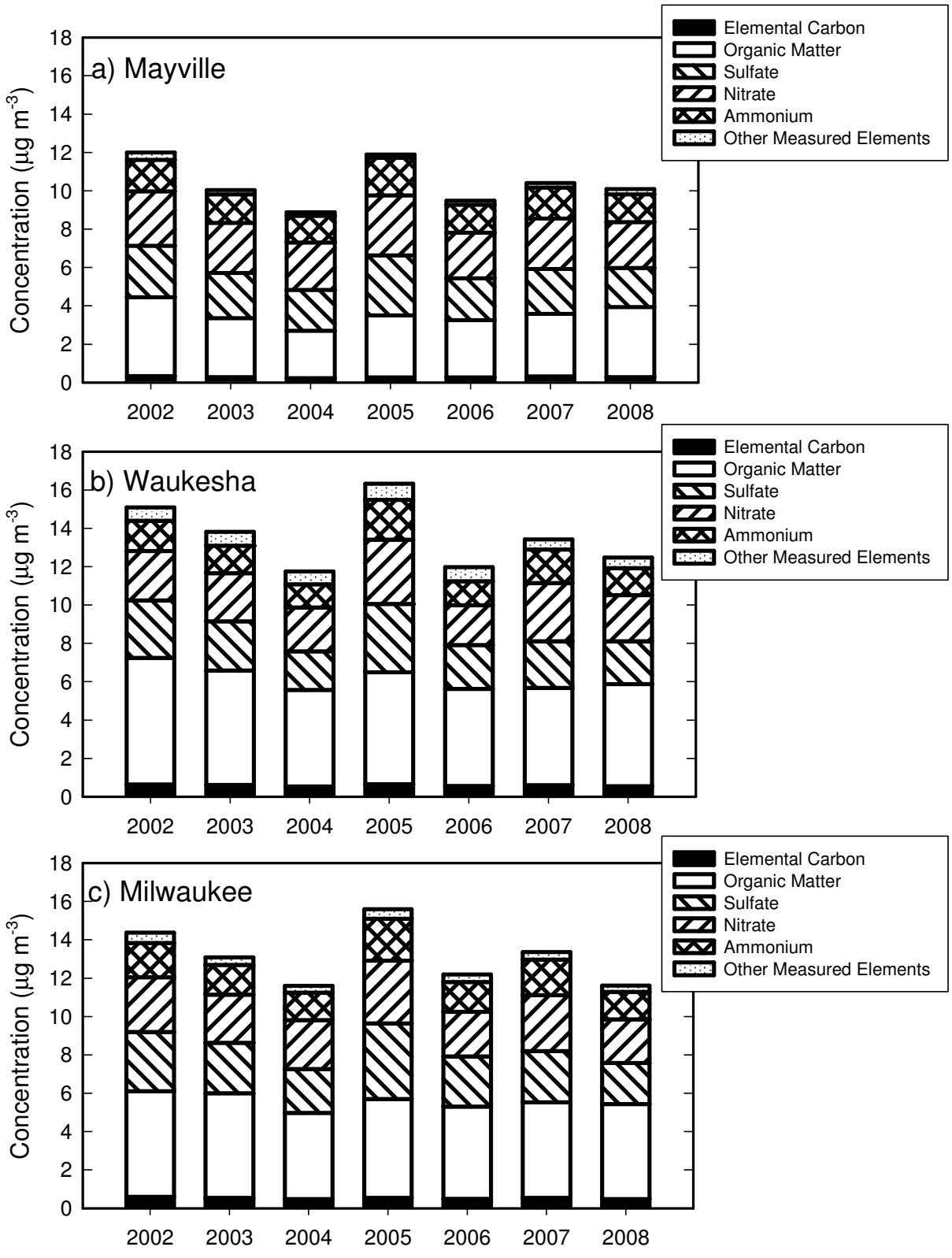

Figure 1. Temporal trends of chemical species concentrations of PM2.5 at each site.

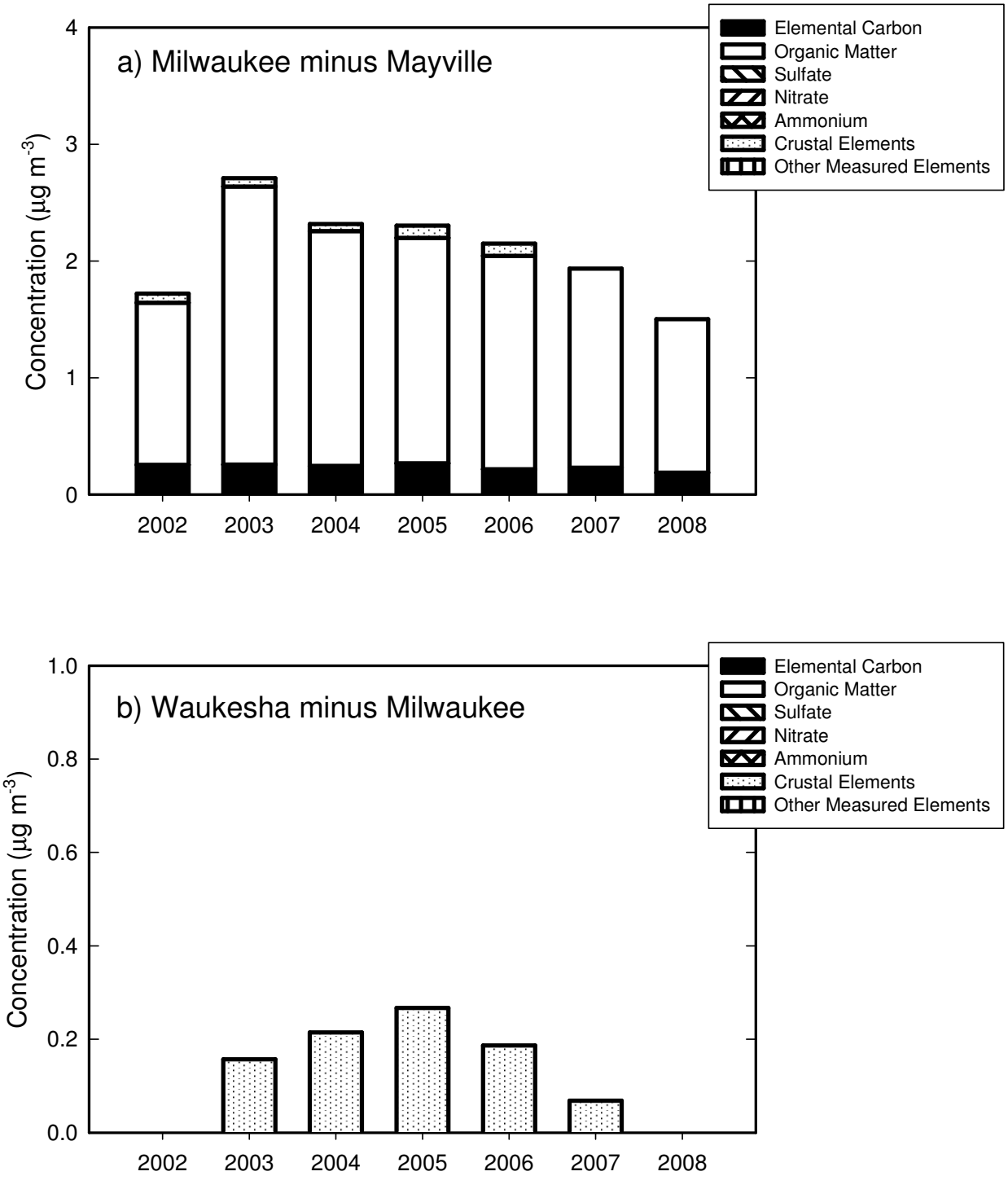

Figure 2. Variations of urban excess of major chemical species in two different sample sites.

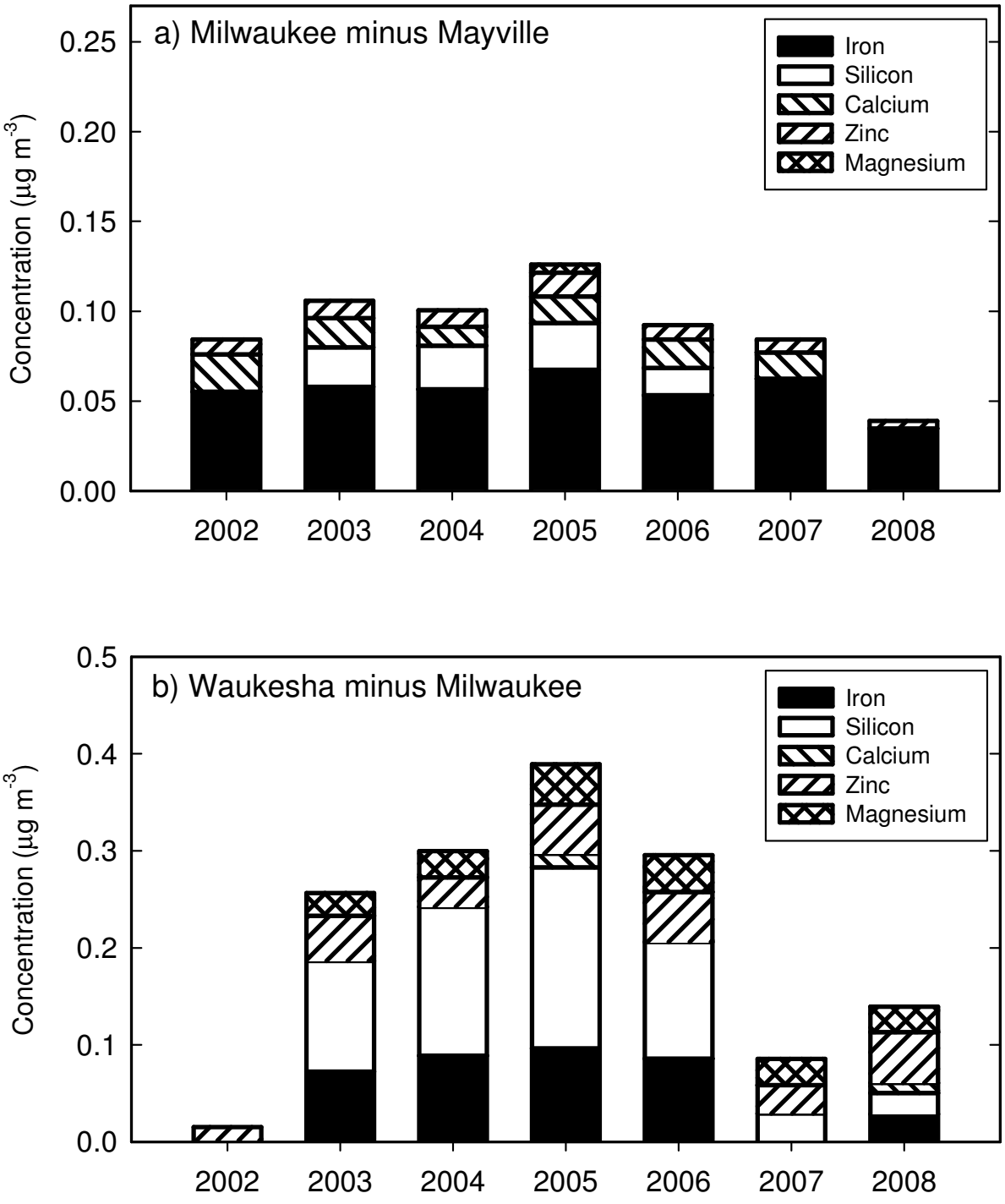

Figure 3. Variations of urban excess for several trace elements in two different sample sites.

Table 1. Summary of regression results for urban excess

	Milwaukee vs. Mayville					Milwaukee vs. Waukesha				
Element	Slope	Slope UNC	Intercept	INT UNC	r^2	Slope	Slope UNC	Intercept	INT UNC	r^2
PM2.5	**0.833**	**0.031**	**3.264**	**0.405**	0.665	**0.909**	**0.025**	-0.036	0.376	0.791
Organic Carbon	0.918	0.042	**1.160**	**0.097**	0.566	**0.721**	**0.036**	**0.603**	**0.126**	0.532
Elemental Carbon	0.929	0.083	**0.267**	**0.028**	0.258	**0.706**	**0.038**	**0.118**	**0.025**	0.492
Nitrate	0.971	0.017	**0.139**	**0.067**	0.899	1.001	0.012	-0.008	0.048	0.951
Sulfate	**1.122**	**0.020**	0.056	0.066	0.899	**1.105**	**0.013**	**-0.156**	**0.047**	0.951
Ammonium	**1.042**	**0.020**	0.070	0.042	0.883	**1.069**	**0.015**	0.026	0.032	0.933
Antimony	**0.021**	**0.040**	**0.004**	**0.001**	0.001	**-0.066**	**0.045**	**0.004**	**0.001**	0.006
Arsenic	**0.192**	**0.058**	**0.001**	**0.000**	0.029	**0.138**	**0.038**	**0.001**	**0.000**	0.035
Aluminum	1.005	0.038	**0.005**	**0.002**	0.662	**0.701**	**0.035**	0.003	0.002	0.532
Bromine	0.700	0.355	**0.004**	**0.001**	0.011	0.782	0.272	**0.003**	**0.001**	0.022
Calcium	1.006	0.051	**0.013**	**0.002**	0.519	**0.563**	**0.039**	**0.013**	**0.002**	0.362
Chromium	**-0.001**	**0.109**	**0.002**	**0.000**	0.000	**0.085**	**0.037**	**0.002**	**0.000**	0.014
Copper	**0.045**	**0.050**	**0.004**	**0.000**	0.002	**0.183**	**0.029**	**0.002**	**0.001**	0.097
Chlorine	**1.430**	**0.080**	0.004	0.002	0.471	**0.333**	**0.039**	**0.007**	**0.003**	0.166
Iron	**1.501**	**0.124**	**0.044**	**0.005**	0.287	**0.268**	**0.026**	**0.045**	**0.005**	0.224
Lead	**0.312**	**0.050**	**0.003**	**0.000**	0.097	**0.060**	**0.025**	**0.003**	**0.000**	0.016
Manganese	**1.790**	**0.312**	**0.005**	**0.001**	0.083	**0.280**	**0.036**	**0.004**	**0.001**	0.145
Magnesium	**0.211**	**0.096**	**0.007**	**0.001**	0.013	**0.020**	**0.016**	**0.007**	**0.001**	0.004
Selenium	**0.437**	**0.062**	**0.000**	**0.000**	0.122	**0.063**	**0.011**	**0.001**	**0.000**	0.089
Titanium	**0.810**	**0.049**	**0.001**	**0.000**	0.429	**0.416**	**0.035**	**0.001**	**0.000**	0.283
Vanadium	**0.222**	**0.057**	**0.001**	**0.000**	0.040	**0.166**	**0.040**	**0.001**	**0.000**	0.047
Silicon	**0.419**	**0.033**	**0.040**	**0.005**	0.303	**0.204**	**0.019**	**0.029**	**0.006**	0.236
Zinc	1.228	0.124	**0.007**	**0.001**	0.214	**0.028**	**0.009**	**0.014**	**0.001**	0.026
Strontium	0.915	0.043	**0.000**	**0.000**	0.559	**0.669**	**0.030**	0.000	0.000	0.585
Sulfur	**1.135**	**0.018**	0.020	0.021	0.912	**1.116**	**0.013**	**-0.076**	**0.016**	0.952
Terbium	**1.408**	**0.129**	**0.000**	**0.000**	0.246	**0.387**	**0.039**	**0.001**	**0.000**	0.216
Rubidium	**0.140**	**0.052**	**0.000**	**0.000**	0.020	**-0.021**	**0.057**	**0.000**	**0.000**	0.000
Potassium	**1.481**	**0.031**	**-0.010**	**0.003**	0.861	**0.726**	**0.011**	**0.005**	**0.002**	0.919
Sodium	**0.369**	**0.069**	**0.021**	**0.004**	0.074	**0.236**	**0.051**	**0.019**	**0.004**	0.056
Zirconium	**0.056**	**0.129**	**0.001**	**0.000**	0.001	**-0.059**	**0.080**	**0.001**	**0.000**	0.001
Sodium Ion	**0.290**	**0.050**	**0.040**	**0.006**	0.085	**0.304**	**0.041**	**0.036**	**0.006**	0.133
Potassium Ion	**1.403**	**0.041**	-0.003	0.003	0.763	**0.757**	**0.015**	**0.005**	**0.002**	0.874

*Bold = |1-slope| > 2 × uncertainty, and Bold = |Intercept| > 2 × uncertainty

Table 2. Summary of mean concentration for each chemical species at three STN sites

	Mayville			Waukesha			Milwaukee		
Element	Average	Slope	Slope UNC	Average	Slope	Slope UNC	Average	Slope	Slope UNC
PM2.5	10.2421	0.0323	0.2134	12.9146	-0.0917	0.3219	11.9217	-0.1448	0.2823
Organic Carbon	1.8081	-0.0102	0.0593	3.0849	**-0.1105**	**0.0477**	2.8050	-0.0448	0.0358
Elemental Carbon	0.2897	-0.0018	0.0072	0.5968	-0.0091	0.0082	0.5259	-0.0122	0.0076
Nitrate	2.6390	-0.0496	0.0514	2.6095	0.0119	0.0904	2.6712	-0.0418	0.0717
Sulfate	2.4039	-0.0675	0.0728	2.5847	-0.0820	0.1040	2.7696	-0.0868	0.1178
Ammonium	1.5709	-0.0099	0.0394	1.5280	0.0054	0.0635	1.6875	-0.0114	0.0562
Antimony	0.0026	**-0.0007**	**0.0003**	0.0025	-0.0006	0.0004	0.0028	-0.0006	0.0006
Arsenic	0.0006	**-0.0001**	**0.0000**	0.0012	**-0.0002**	**0.0000**	0.0008	**-0.0001**	**0.0000**
Aluminum	0.0116	0.0009	0.0011	0.0209	**-0.0024**	**0.0008**	0.0165	0.0005	0.0014
Bromine	0.0017	0.0001	0.0000	0.0021	**0.0001**	**0.0001**	0.0048	**0.0008**	**0.0004**
Calcium	0.0264	-0.0009	0.0010	0.0469	-0.0022	0.0012	0.0396	**-0.0031**	**0.0011**
Chromium	0.0010	0.0000	0.0002	0.0028	-0.0001	0.0001	0.0020	0.0000	0.0002
Copper	0.0018	0.0003	0.0002	0.0131	**-0.0027**	**0.0008**	0.0035	-0.0003	0.0002
Chlorine	0.0102	**0.0020**	**0.0007**	0.0314	**0.0040**	**0.0010**	0.0207	**0.0027**	**0.0012**
Iron	0.0287	-0.0001	0.0010	0.1435	-0.0041	0.0081	0.0840	-0.0021	0.0023
Lead	0.0024	**-0.0003**	**0.0001**	0.0070	-0.0003	0.0004	0.0039	**-0.0005**	**0.0002**
Manganese	0.0012	**-0.0001**	**0.0001**	0.0105	0.0002	0.0004	0.0063	-0.0005	0.0004
Magnesium	0.0041	-0.0005	0.0004	0.0340	0.0020	0.0021	0.0069	**-0.0008**	**0.0004**
Selenium	0.0004	-0.0001	0.0000	0.0010	**-0.0002**	**0.0001**	0.0005	**-0.0001**	**0.0000**
Titanium	0.0011	**-0.0005**	**0.0001**	0.0031	**-0.0008**	**0.0002**	0.0020	**-0.0007**	**0.0002**
Vanadium	0.0003	0.0000	0.0000	0.0007	0.0000	0.0001	0.0006	0.0000	0.0001
Silicon	0.0458	-0.0024	0.0035	0.1569	-0.0169	0.0105	0.0616	**-0.0074**	**0.0025**
Zinc	0.0070	-0.0001	0.0002	0.0550	0.0027	0.0029	0.0155	-0.0008	0.0007
Strontium	0.0003	-0.0001	0.0000	0.0008	0.0000	0.0001	0.0007	0.0000	0.0001
Sulfur	0.8163	-0.0224	0.0256	0.9007	-0.0186	0.0353	0.9358	-0.0255	0.0361
Terbium	0.0004	0.0000	0.0002	0.0014	-0.0001	0.0005	0.0009	-0.0001	0.0004
Rubidium	0.0002	0.0000	0.0000	0.0001	0.0000	0.0000	0.0002	0.0000	0.0000
Potassium	0.0467	**0.0027**	**0.0012**	0.0844	0.0050	0.0036	0.0720	0.0010	0.0041
Sodium	0.0167	-0.0032	0.0017	0.0334	0.0004	0.0030	0.0233	-0.0034	0.0023
Zirconium	0.0005	0.0000	0.0001	0.0008	-0.0001	0.0001	0.0007	0.0000	0.0001
Sodium Ion	0.0436	-0.0092	0.0078	0.0584	-0.0110	0.0104	0.0698	-0.0102	0.0083
Potassium Ion	0.0288	0.0060	0.0018	0.0540	**0.0119**	**0.0035**	0.0518	0.0054	0.0036

*Bold = |slope| > 2 × uncertainty

Positive Matrix Factorization (PMF) Analysis

Figure 4 shows the identified source profiles and their seasonal average contributions across the sites. The PMF model identified six common sources discussed below in which their source profiles are remarkably stable and similar between sites. Average source contributions to total $PM_{2.5}$mass for each site is indicated in the following parentheses: secondary nitrate (approximately 37% for Mayville, 30% for Waukesha, and 33% for Milwaukee), secondary sulfate (approximately 31% for Mayville, 28% for Waukesha, and 31% for Milwaukee), biomass burning (approximately 12% for Mayville, 17% for Waukesha, and 10% for Milwaukee), mobile (approximately 9% for Mayville, 8% for Waukesha, and 12% for Milwaukee), resuspended soil (approximately 6% for Mayville, 5% for Waukesha, and 4% for Milwaukee), and road salt (approximately 2% for Mayville, 3% for Waukesha, and 2% for Milwaukee). The secondary nitrate is characterized by high loading of nitrate and ammonium concentrations with distinctive seasonal patterns of high winter peaks, indicating low temperature and high humidity meteorological conditions in this study region help enhance the formation of secondary nitrate particles. In contrast, the secondary sulfate is identified by high concentrations of sulfate and ammonium with high summer peaks, representing the formation of secondary sulfate aerosols is enhanced during the summer when photochemical reaction of sulfur dioxide to sulfate is highest. The secondary nitrate and secondary sulfate are predominant sources making up 58% to 67% of the total $PM_{2.5}$ mass. Biomass burning is represented by high concentrations of potassium and OC which are indicator species for biomass burning and wood smoke. This source does not show strong seasonal variations in this analysis. The mobile source is dominated by high loading of OC and EC concentrations. Resuspended soil had high concentrations of aluminum, silicon, iron, and calcium and displayed weak seasonal patterns. Road salt is identified by very high concentrations of chloride and sodium, and largely contributed largely to the total $PM_{2.5}$ in the winter.

Figure 5, 6 and 7 show a comparison of the estimated daily source contributions and urban excess estimates for the same sources across the sites. The secondary nitrate and secondary sulfate have strong correlations between sites, especially between Waukesha and Milwaukee. This strong relationship suggests these secondary formed particles can be significantly influenced by regional sources and can lead to the regional PM2.5 episodes in Wisconsin.

Site-specific primary emission sources are resolved from the PMF analysis as 4% industry for Mayville, two types of industry sources (6%) and copper emission (3%) for Waukesha, and separated diesel emission (3%), industry (1%), and bromine emission (4%) for Milwaukee. The identified industrial sources are separated into two types which include type-1 with high concentrations of iron and manganese and chromium in the Waukesha and Milwaukee site and type-2 with high zinc, magnesium, lead, iron, silicon and sulfate concentrations in the Waukesha and Mayville site. Steel processing has a high covariance of iron, manganese, and chromium [*Lee and Hopke*, 2006], thus type-1 industrial sources can be represented by local primary steel processing emissions. It is not clear whether the type-2 industrial source has one dominant source contribution, but this source can represent the impact of several primary sources because non-ferrous metal and steel process have high signatures of zinc and iron and cement kilns and limestone quarries have high emissions of silicon [*Lee and Hopke*, 2006]. Copper emission source was identified in the Waukesha site with high concentrations of copper, OC, and sulfate. A metal part fabricator is located near the Waukesha STN site and have a strong influence on the PM2.5 mass as one distinctive source. For the Milwaukee site, the diesel emission source broke off from the mobile source showing high EC, zinc, lead, iron, and calcium concentrations and high weekday contributions. In general, higher EC than OC concentrations is considered to be a signature of heavy-duty diesel vehicle emission. Other metals such as lead and calcium are emitted from diesel-powered vehicles [*Gertler et al.*, 2002]. Therefore, this identified source profile is likely to be diesel emission. In the Milwaukee site, the bromine source was identified by high bromine concentrations with unique peaks in the summer time. Because bromine is normally used as an additive in lubricating oil [*Polissar et al.*, 1998], it is likely the bromine source can be considered emissions from primary mobile combustion including ships that use piston chambers in which fuel and lubricant are mixed and burned together. However, further research is required to better identify this source correctly.

As seen in Figure 7, the major excess of the sources between Milwaukee and Mayville is in primary emissions including mobile and bromine sources and secondary sulfate. The excess source contributions in Waukesha compared to Milwaukee is mainly biomass burning, industry, and copper sources, while the excess of the sources in Milwaukee compared to Waukesha is caused by mobile and bromine sources. The PMF source identification and excess results are evaluated with the conclusion that the regional sources, such as secondary sulfate and nitrate,

contribute equally to the total $PM_{2.5}$ mass in Milwaukee and Waukesha counties, and thus controls and restrictions of these sources could be implemented to help lower the $PM_{2.5}$ concentration and bring these counties into attainment.

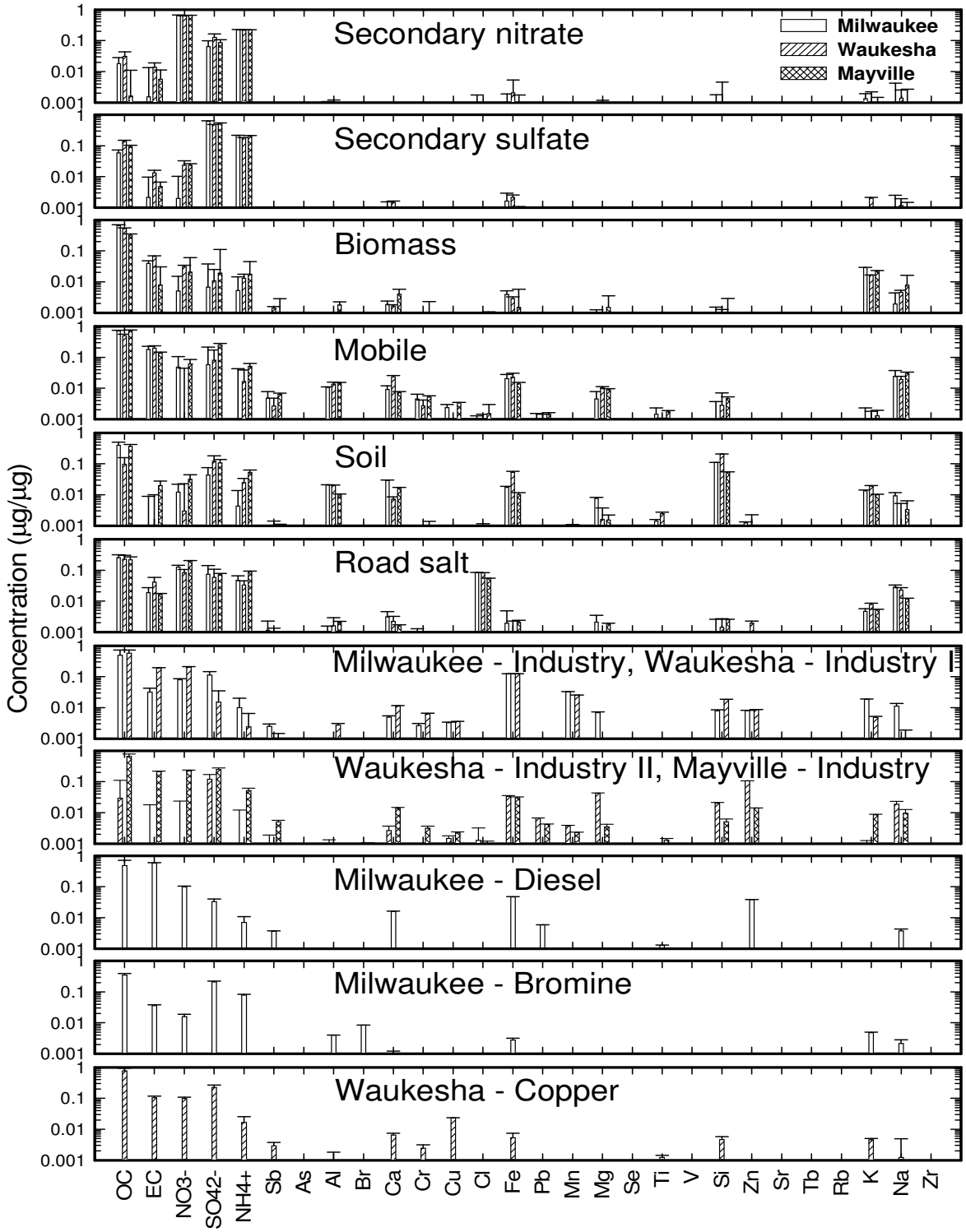

Figure 4. Source profiles from PM2.5 samples measured at Milwaukee, Waukesha, and Mayville sites.

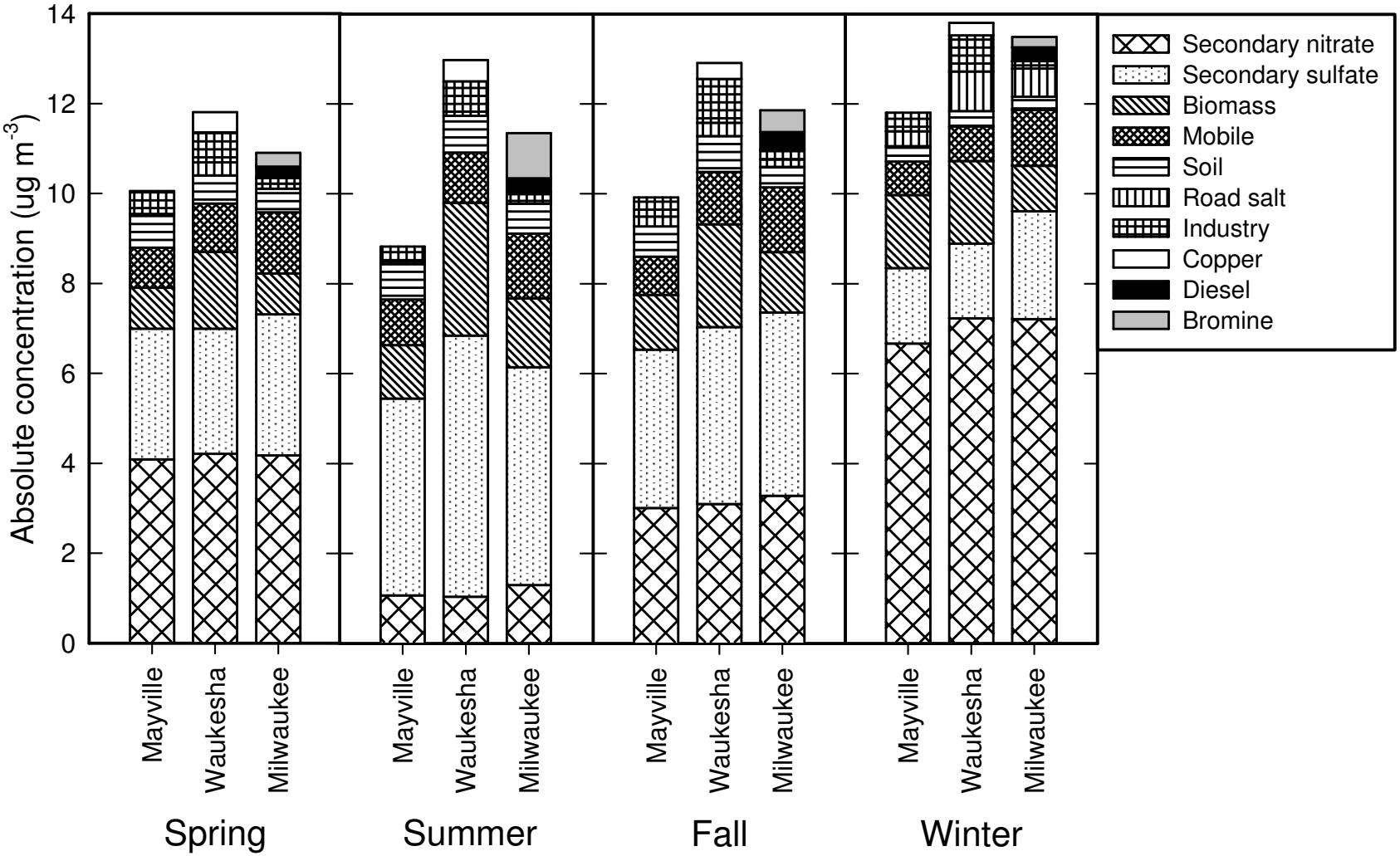

Figure 5. Seasonal source contributions to PM2.5 concentrations at Mayville, Waukesha, and Milwaukee sites.

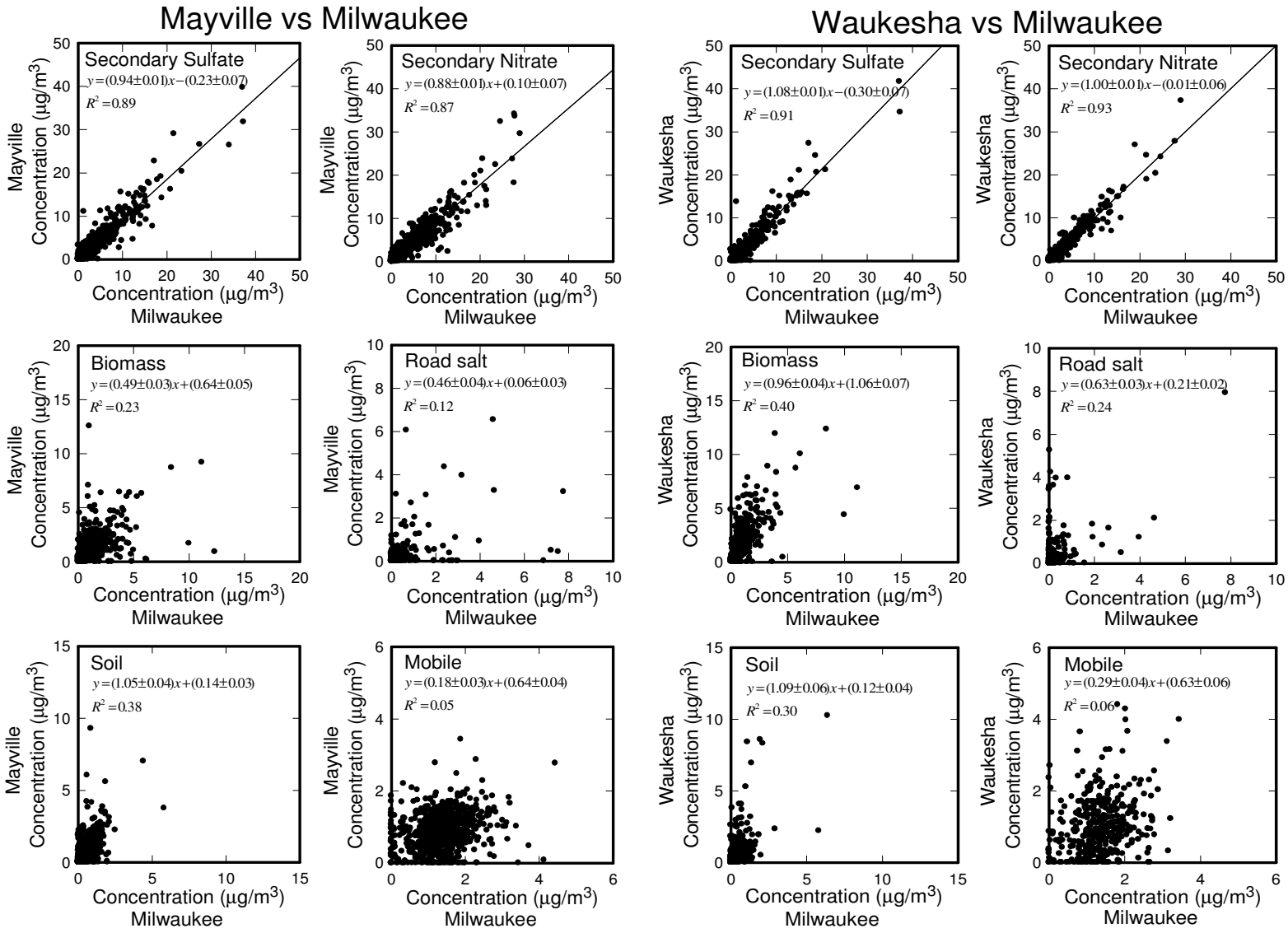

Figure 6. Comparison of PMF deduced source contributions between sites.

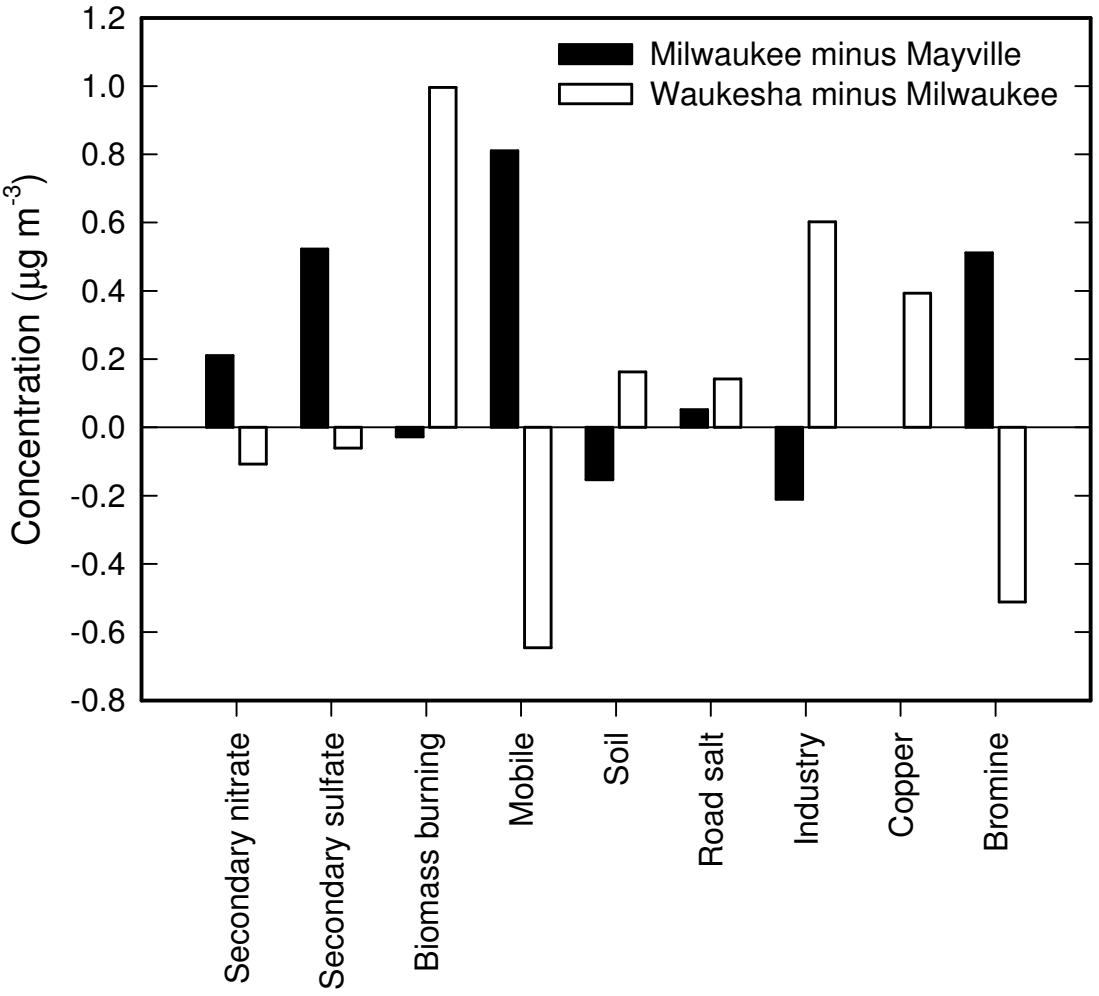

Figure 7. Urban excess of PMF deduced sources between sites.

PSCF Analysis

The residence time of the back trajectories calculated from 2002 through 2010 at the three receptor sites (Madison, Milwaukee and Waukesha) shows that the air masses moving in southern Wisconsin travel predominantly from the northwest and the southwest. Figure 8a shows the PSCF plots of sulfate concentrations in Milwaukee and indicate the Ohio River Valley area and adjacent states as potential source areas and pathways contributing to the excess of sulfate in southern Wisconsin. This suggests the SO2 emitted from coal fired power plants in the valley is transformed into sulfate aerosols when air parcels are transported over long-distances and consequently lead to an increase of PM2.5 sulfate in the southern Wisconsin. Figure 8b shows the high PSCF nitrate values in Milwaukee originated in the Ohio River Valley, mostly along the Indiana-Illinois border. Ambient nitrate is formed through oxidation of NO_x which is emitted from mobile and stationary sources such as coal-fired power plants. Because many emission sources are located along the Indiana-Illinois border, this area can be seen as high source probability region for an increase of nitrate in southern Wisconsin. As discussed in a previous section, the comparison of daily source contributions of secondary sulfate and secondary nitrate factors derived from the PMF at each site, especially between Waukesha and Milwaukee, shows there is a strong correlation between each site for these estimated source contributions, suggesting substantial impacts of regional sources at this receptor area. This is well supported by the PSCF probability maps.

Exceedance of PM2.5 ambient standards occur across the Wisconsin area regardless of season but are more frequent during winter. To identify the likely source locations of the elevated PM2.5 concentrations during winter, joint-PSCF analysis was conducted using 24-hour PM2.5 mass data based on 1-in-3 day time intervals from 2002 through 2010 at three FRM sites; Madison, Waukesha, and Milwaukee in Wisconsin. The results of joint-PSCF revealed the highest source probabilities for the elevated PM2.5 in Wisconsin were located along the confluence of the central area of the Mississippi River, Illinois River, Missouri River and the Arkansas river in Oklahoma when the threshold criteria of the upper 25% of PM2.5 concentrations were applied as the wintertime PM2.5 episodes. The Arkansas River in Oklahoma appeared to be the main source region when the threshold criteria were 30 $\mu g/m^3$ of PM2.5 mass during wintertime PM2.5 episodes. In northern sites of the Midwest, wintertime

PM2.5 during episodes have been strongly enriched in ammonium nitrate and have been driven by stagnant air masses accompanied by high pressure, slow wind speed, high relative humidity without a sudden increase of local emissions [*LADCO, 2009*]. In general, low temperature and high humidity air conditions increase the formation of ammonium nitrate particles while shifting the equilibrium system of NH_3^- and HNO_3 toward the particle phase [*Seinfeld and Pandis, 1998*]. Other than the specific meteorological conditions, ammonia availability can play a significant role in the formation of ammonium nitrate particles. The potential source regions for PM2.5 mass shown in Figure 9ab are linked to a high ammonia emission zone that includes animal confinement facilities and fertilizer application to agricultural croplands [*Lee and Hopke*, 2006]. Therefore, the elevated PM2.5 mass observed in in Wisconsin winters are likely influenced by air masses and path trajectories which bring enrichments of ammonia and the meteorological conditions discussed above.

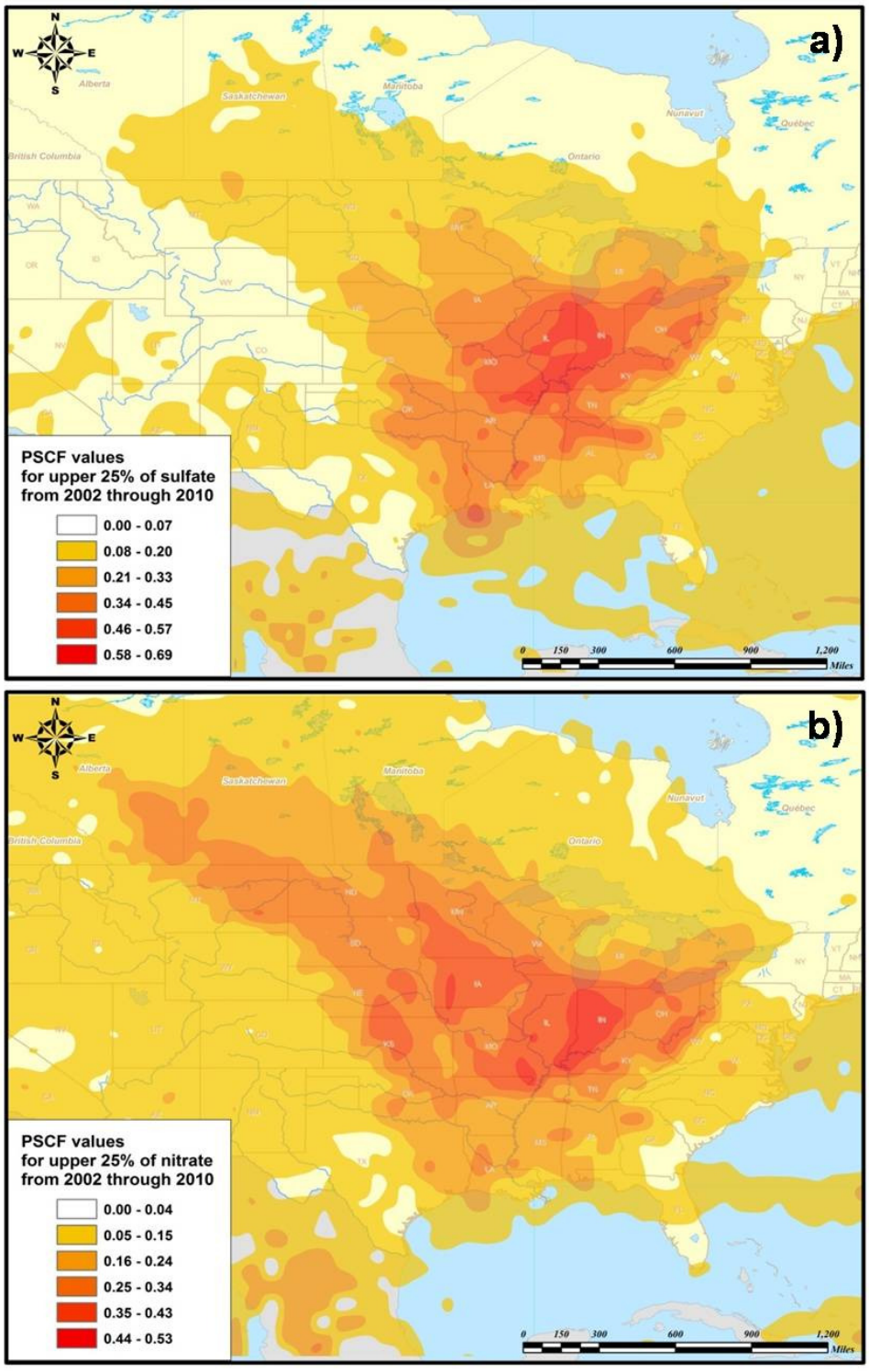

Figure 8. Probable source locations for upper 25% of sulfate and nitrate concentrations measured in Milwaukee during the entire study period.

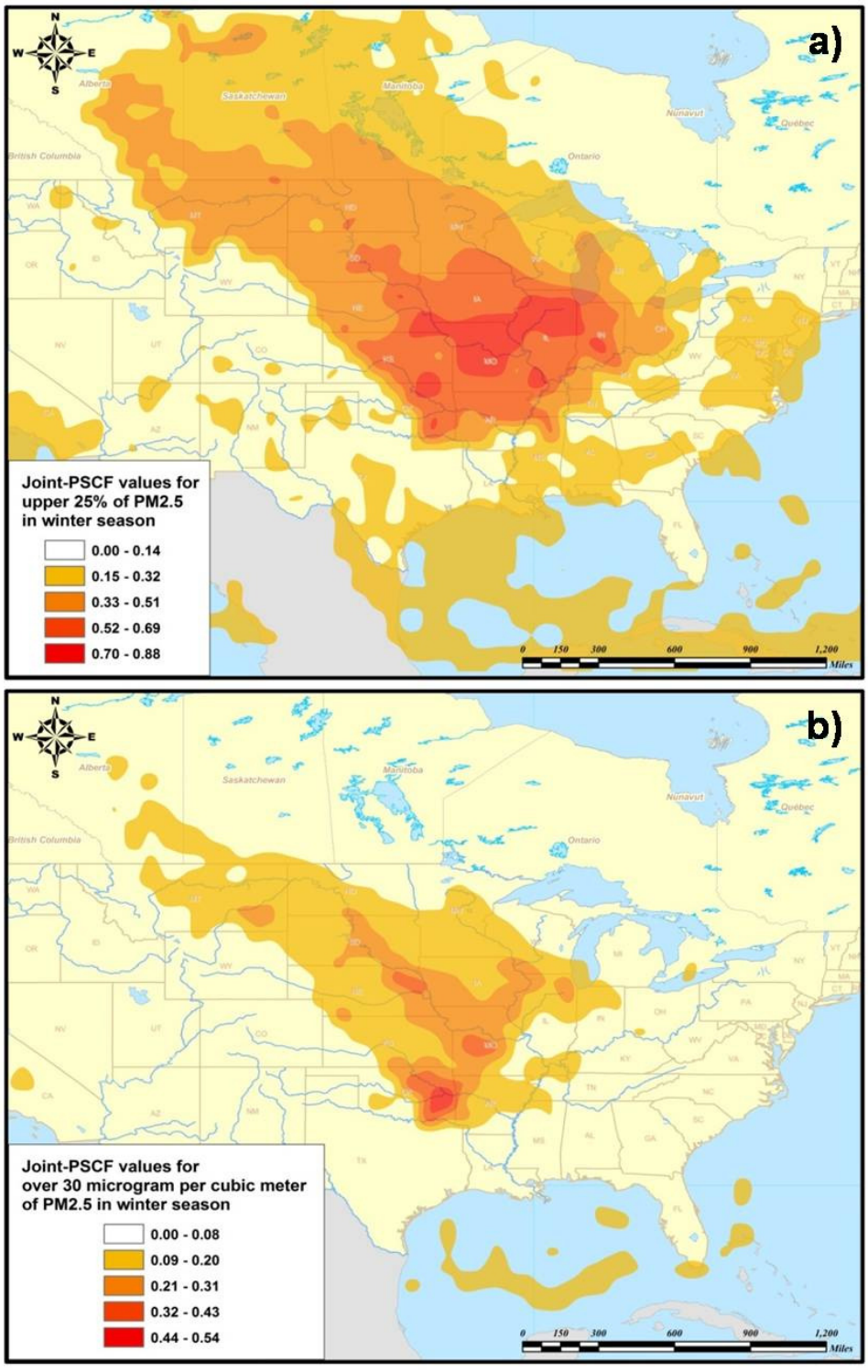

Figure 9. Probable source locations for upper 25% and greater than 30 µg m-3 of PM2.5 mass concentrations measured in Madison, Milwaukee, and Waukesha during the entire winter season from 2002 through 2010.

Summertime Intensive Measurements

Averaged hourly measurements are reported from July 15 through August 15, 2010. Discontinuities of the sample record occur during QA/QC spike and blank calibration checks performed on the API SO2 monitor, the TSI and AIM insturments. Additionally, approximately two days (July 28 and July 29) of anion data did not meet quality assurance criteria due to an equipment failure, and are not included in the reported values. Aethalometer tape advances occurred approximately three times per day, with each advance requiring 20 minutes of sample time; hourly averages were calculated using available data during the hour when the tape advanced. A time series of hourly average concentrations are plotted in Figure 10. No clear trends were observed between the individual data sets; however, several events are noteworthy. Sulfur dioxide spikes during the weeks of July 19th and July 26th had corresponding sulfates spikes showing SO2 was being oxidized and the fact that both species were present indicates the SO2 in these events was from a localized source. During the week of August 2nd, sulfate levels are elevated but no corresponding SO2 peak was observed, indicating the sulfate is likely from a regional (or beyond the region) source of SO2 which had been oxidized during transport. In addition, sulfate and nitrate increases were observed during the days around August 2nd, corresponding with an increase in ammonium concentration, these trends lead to the conclusion of longer range transport of ammonium-sulfate and ammonium-nitrate. Black carbon (BC) concentrations showed daily variability associated with expected traffic patterns, including deceased weekend concentrations. This indicates BC concentrations in the Milwaukee region are very dependent on local emissions. On two dates BC spikes correspond well with other observed elevated concentrations. First, on July 26 a BC spike corresponded well with the SO2 and Sulfate spikes, indicating the BC elevation was not likely a result of only traffic emissions, but rather a nearby point source (or point sources). Second, on August 10th a BC spike corresponded with a nitrate spike, which was likely due to nearby road way diesel vehicle emissions.

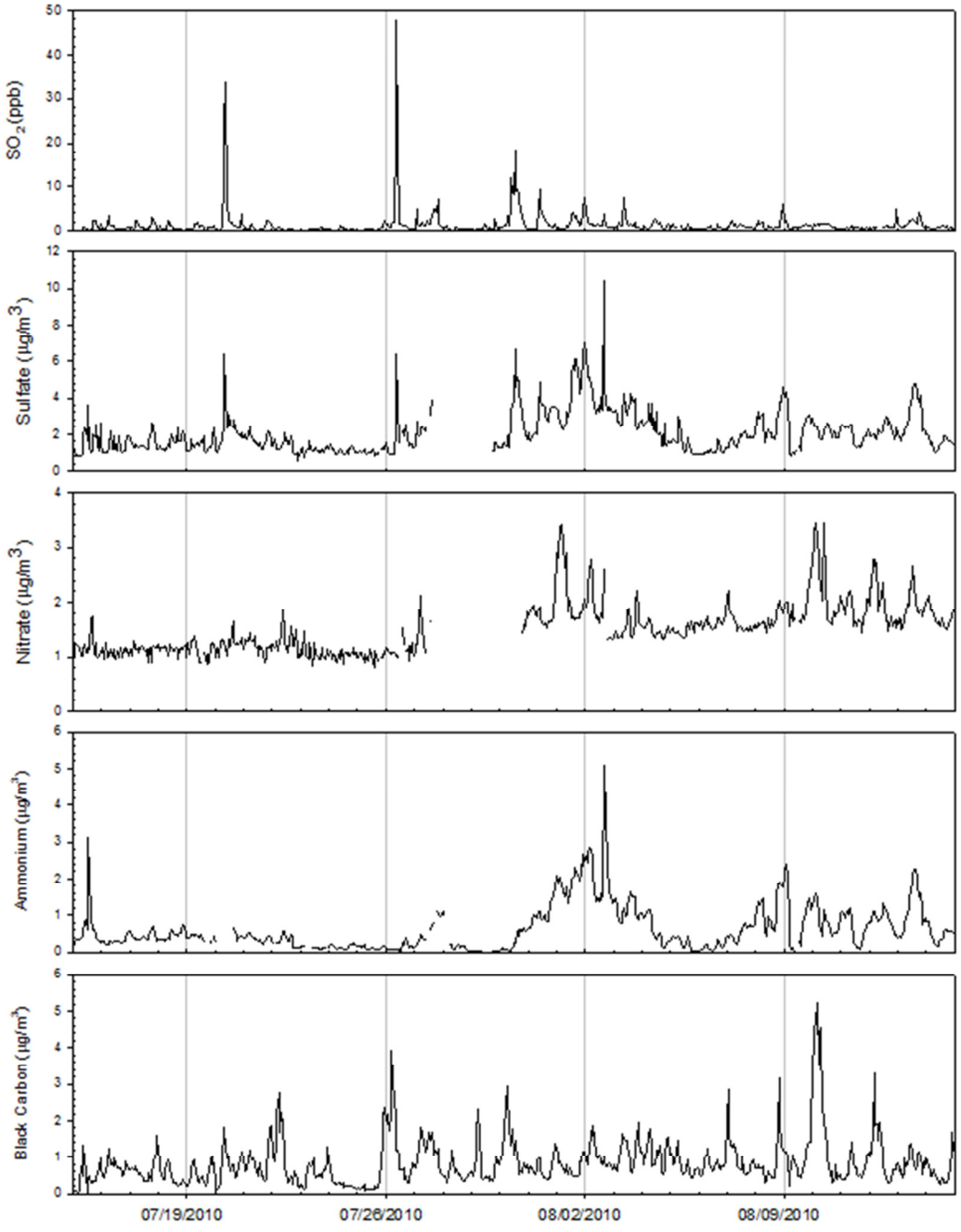

Figure 10. Hourly average concentration at the WDNR-SER site in Milwaukee, WI, collected during July 15 through August 15, 2010.

For the winter intensive measurements, Figure 11 shows CFA results for nitrate and sulfate concentrations at Mayville. Red regions on the map indicate higher concentrations at the receptor sites during windy conditions. This indicates they are either potential source regions themselves, or they lie on the path between a potential source region and the receptor site. The figure shows potential source regions of nitrates mainly from the southwest. Sulfates are from the south, with source regions towards the southwest and the southeast. This is consistent with agricultural and industrial source locations.

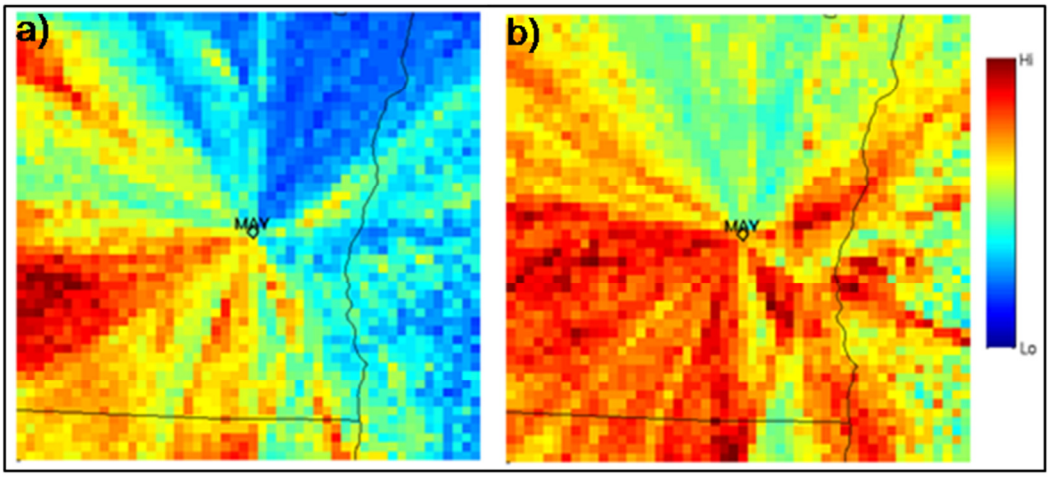

Figure 11. CFA analysis for winter nitrate (a) and sulfate (b) data from Mayville.

For the summer intensive measurements, Figure 12 shows CFA results for black carbon and sulfate concentrations and for nickel particle counts from the Aerosol Time-of-Flight Mass Spectrometer (ATOFMS) in Milwaukee. The black carbon and nickel are from sources south of the measurement site, whereas potential source regions for sulfate are more to the southeast. The plots are consistent with elevated levels of black carbon and nickel from local sources due to stagnation events, and elevated levels of sulfate are due to transport from industrial regions to the southeast of Milwaukee.

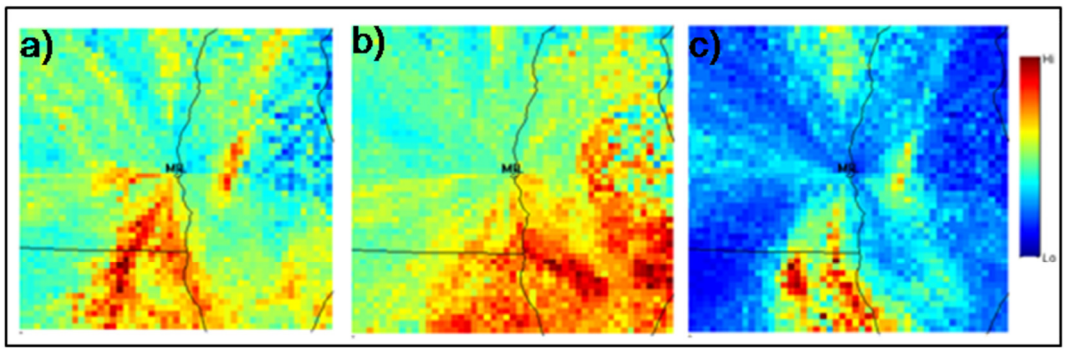

Figure 12. CFA analysis for summer 2010 at Milwaukee for black carbon (a), sulfate (b), and nickel (c).

For the summer intensive measurements, a Eulerian pollutant transport was calculated using the Comprehensive Air quality Model with eXtensions (CAMx), [*ENVIRON 2011*], version 5.40. This was run on WRF domains 2 and 3 (resolution 9 and 3 km) with the first 18 of 41 vertical levels using the O'Brien vertical diffusion coefficients. The simulations were performed for nickel and NOx as passive tracers for local sources and transport.

The US Environmental Protection Agency's National Emissions Inventory (NEI) for 2008 was applied. We used version 1.5, released on May 16, 2011, for point, non-point, on-road and non-road emissions. Large point sources were simulated in CAMx using the Plume-in-Grid method which uses puffs to represent individual plumes as long as they remain smaller than the grid cell. Small point sources were included in the two counties near the receptor site (Milwaukee and Waukesha). Area sources were simulated in CAMx, using a uniform spatial distribution within each Federal Information Processing Standard (FIPS) geographical area code.

The results suggest there are distinct sources of SO2, nickel, vanadium and BC. The main impacts of SO2 are from large, local, point sources to the south of the measurement site. Although the SO2 plumes are associated with some nickel and vanadium, they are not the main source of these pollutants. Nickel and vanadium plumes are associated with calm episodes as well as westerly to southwesterly winds. These are likely associated with point sources in the Menomonee valley south of the measurement site.

Ship emissions from the port of Milwaukee had an impact of 2.8% for nickel and 11.8% for NOx in the simulations using the 2008 NEI. There are significant uncertainties in the inventories

suggest the impact level is underestimated for nickel, but possibly overestimated for NOx. Simulations were also performed from ship tracks along the lake, but these were not found to have a significant impact at the measurement site. Overall, this suggests the impact of ships on fine particle concentrations is below 10%.

Black carbon is associated mainly with transport from the urban section south of the measurement site. The emission inventory and simulations indicate that traffic represents the most significant source of BC. Nickel and vanadium particle counts were at average levels during high black carbon episodes, suggesting there are either joint emissions or spatial overlap of the sources.

Time series analysis suggests as a first approximation, black carbon emissions can be expected to follow NOx emissions. This suggests they are predominantly emitted from local mobile sources. Ships can be expected to contribute potentially up to 10% of black carbon because they emit near the surface 24hrours per day and are located near the urban center. This leads to emissions at night and in the early morning during stable shallow boundary layer conditions relatively close to the measurement site.

Synoptic analysis and classification

Figures 13 and 14 show frequency and windrose maps for the 8 clusters. While there are more west winds, this region experiences winds from all directions over extended time frames. The algorithm accounts for wind speed as this is an important parameter for air pollution dispersion. Some of the clusters therefore clusters are differentiated between strong and weak winds, as seen in clusters 6 and 7.

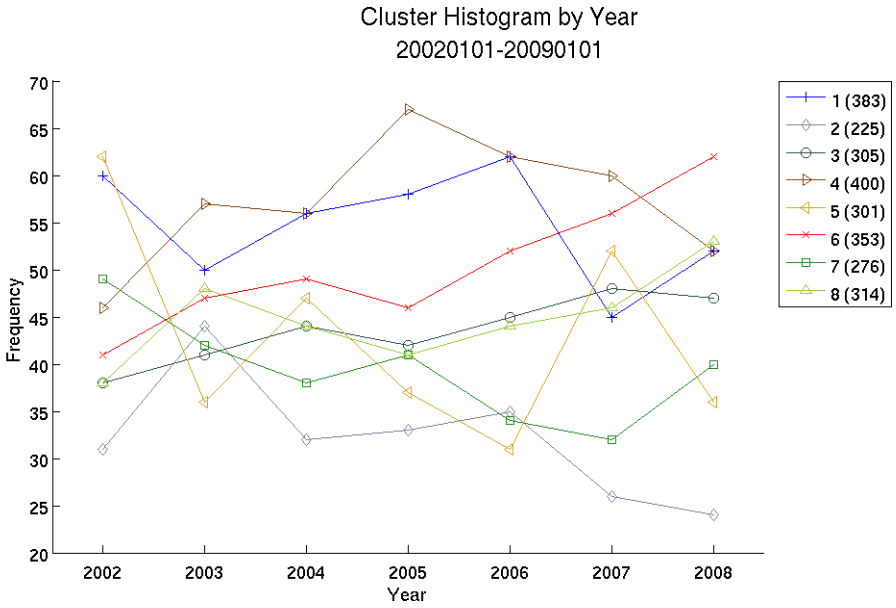

Figure 13. Annual frequency distribution of clusters.

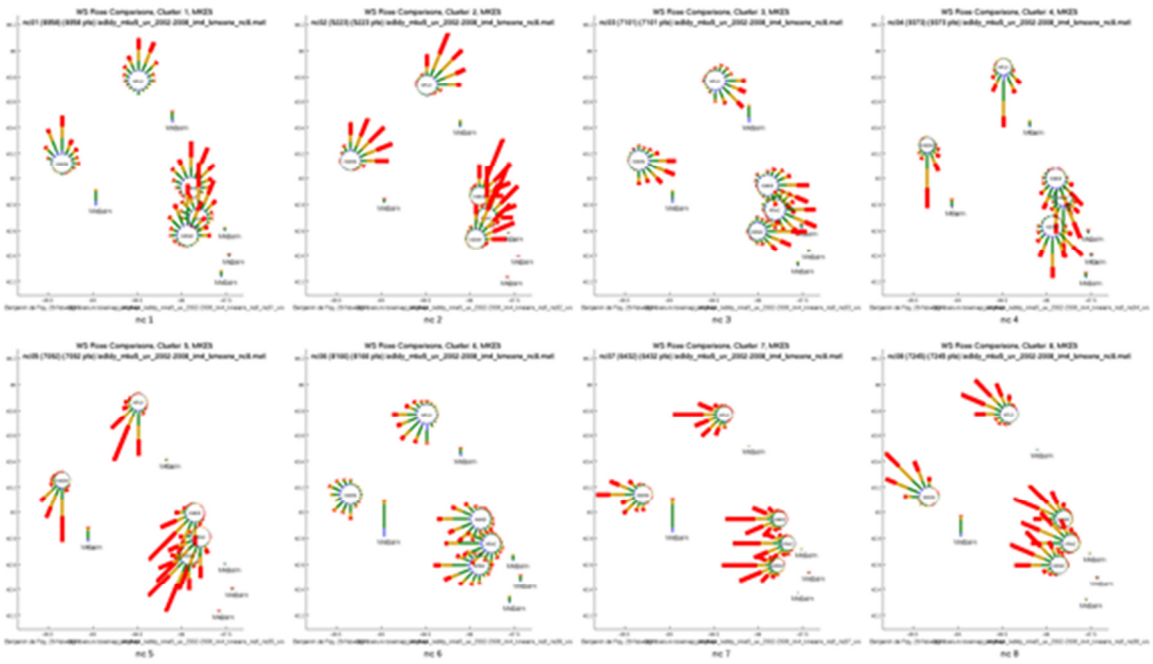

Figure 14. Windrose maps of the 8 clusters of daily averaged wind speed and direction.

ATOFMS Measurements and Results

Metal Ions in Particles

The metal ions present in single-particle mass spectra were counted as peak area associated with the metal ion integrated over hour sampling times. The timelines generated were investigated with Principle Component Analysis (PCA) to identify correlated metals. In the PCA, cadmium and antimony were often correlated, as were selenium and molybdenum. At times, all 5 metal ions would correlate, suggesting they are related in terms of sources. Timelines for these metals support this conclusion (Figure 15).

The timelines shown in Figure 15 suggest there is a local source for the metals and the SO2 data supports the idea that power plants could be contributing to emissions of these metals at certain times. This is further supported by the windrose maps in Figure 14. The windroses for molybdenum are shown in Figure 16. The other metals in Figure 15 have similar windroses.

All five metals shown in Figure 15 were often detected during calm wind events. During the highest 10% of the concentrations, based on peak area, the wind was coming from the WSW. This suggests a local source close to the sampling site located to the WSW of the site. Lower concentrations of metals detected could be from local sources or represent background levels.

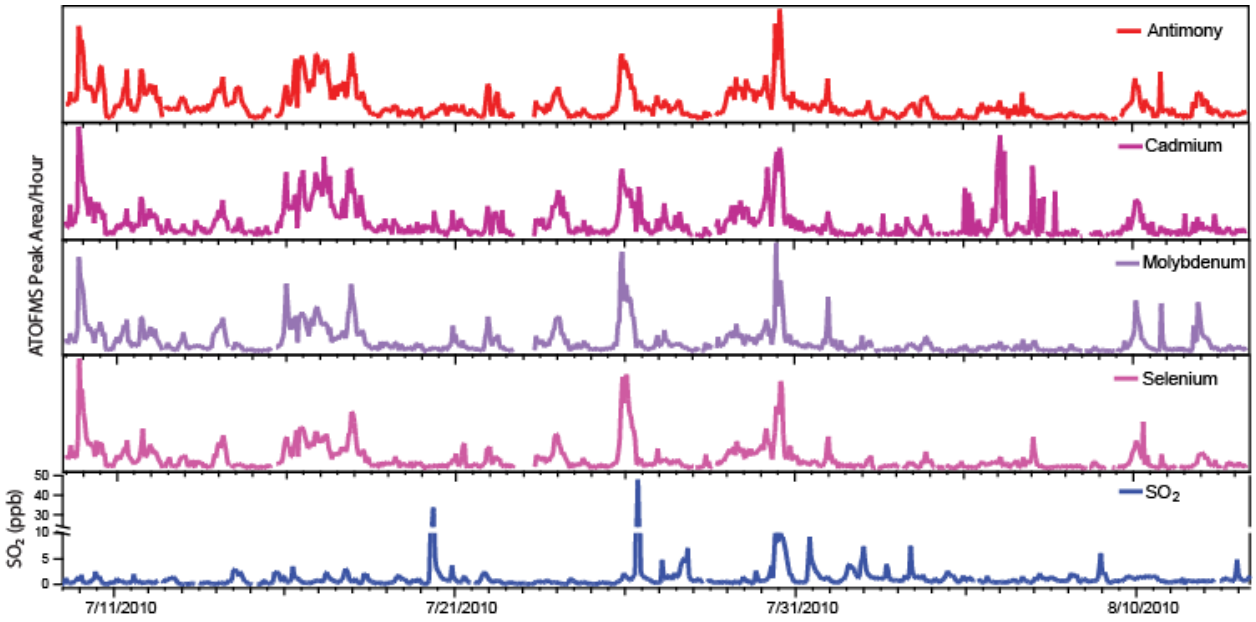

Figure 15. Timelines for the four correlated metals, Mo, Se, Sb, and Cd, along with PM 2.5, and SO2.

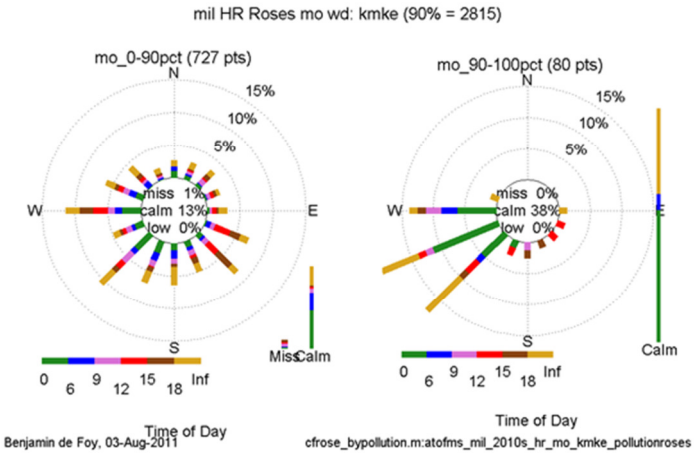

Figure 16. Wind rose of the lowest 90% and highest 10% concentrations for trace Mo observed in single particles. The bar at the bottom of the figure shows the time of day that corresponds to the various colors in the roses, while the bar on the right depicts the percentage of calm winds during sampling.

Bromine in Particles

Particle data collected in Milwaukee from 2002 to 2009 (through the STN network) has shown an increase in bromine, especially during summer months, as seen in Figure 17.

During the summer of 2010 bromine particles were detected and the size distribution of these particles extended to larger particle sizes (~>1 µm) than the overall distribution of sampled particles, indicating larger particles were more likely to contain bromine relative to smaller particles (Figure 18).

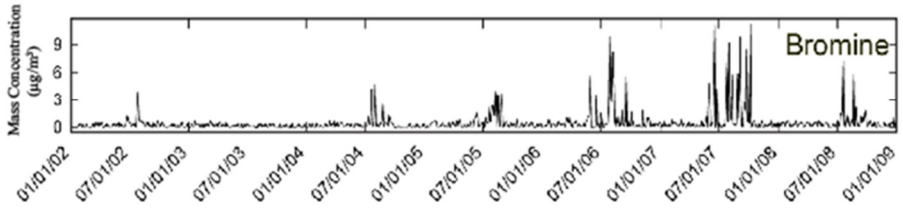

Figure 17. Bromine STN data in Milwaukee, WI.

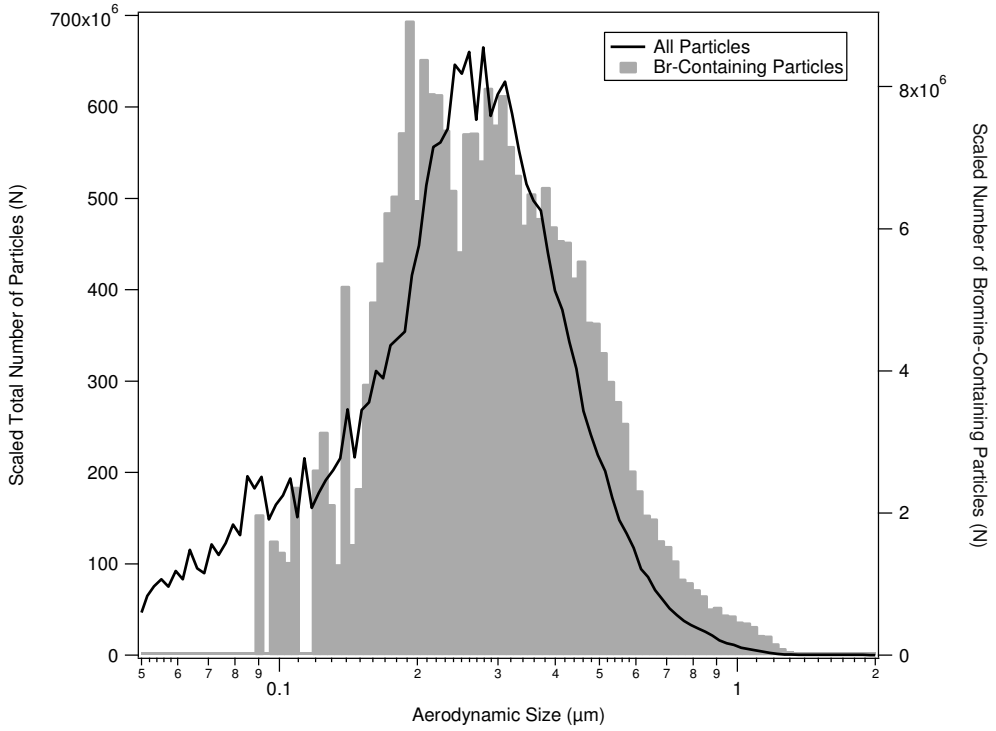

Figure 18. Raw size distributions showing the number distribution of sampled particles and Br-containing particles during the summer of 2010.

The size mode particle spectra have very different characteristics. Smaller particles contain organic fragments, a feature resulting from combustion. Average spectra of larger particles suggest some of the bromine may be crustal in origin, as it resembles dust. Large particles are present whenever bromine-containing particles are observed, and there are no dramatic spikes in the number of large bromine particles detected. On the other hand, the small bromine-containing particles have a much more variable timeline and have dramatic increases in particles detected. This suggests, even if some bromine is present in the form of dust, there is another local source of bromine. This is also supported through wind roses for bromine (not shown).

Source Apportionment using Multiple Sites and Synoptic Regime Information

Two extensions were applied to the existing work in Bayesian PSA:

1. Addressing pollution measurements from multiple sites in the same region and fitting common sources, yet allowing contribution levels to vary by site.

2. Exploring the relationship between synoptic regimes, or large-scale weather patterns, and pollution contributions, and whether this additional information can be exploited to better estimate the contributions.

A Bayesian model was used for the first extension. For the second, a post hoc statistical analysis on the estimated profiles, as well as a Bayesian model which may potentially help include the information about synoptic regimes in the estimation process was employed. Bayesian inference was performed using MCMC code written in MATLAB to generate draws from the posterior distributions.

Multiple Locations

Other than having, on average, narrower credible intervals, the posteriors of the elements of the Λ matrix estimated using data from multiple sites match those estimated from the data for a single site very closely. The correlations of posterior means, medians, and the endpoints of equal-tail 95% credible intervals are all above 0.99, and very few of the posterior means differ by more than 0.01 between the two estimates. The estimated Λ matrices using just the Milwaukee data and using all three sites are found in Tables 3 and 4, respectively.

The estimated contribution levels for all three sites are plotted in Figure 19. Major tick marks are placed at January 1 of each year. Because the details of these results are not of primary interest in this project, we will not discuss them at length; however, we note two interesting features of the estimated contributions. There is a clear seasonal pattern in the contribution levels of the Secondary Nitrate source, with higher contribution levels during the winter months. In addition, we note the relatively low contributions by industry and high contributions by soil dust at the Mayfield site, which is more rural than either of the Milwaukee and Waukesha sites.

Table 3. Posterior mean of the Λ matrix estimated from the Milwaukee site.

	Sec. Nit.	Sec. Sulf.	Biomass	Mobile	Soil	Road Salt	Industry	Bromine	Diesel
OC	0.03459	0.07302	0.61164	0.88001	0.54950	0.48498	0.49926	0.52894	0.30406
EC	0.00487	0.00757	0.04149	0.01233	0.04179	0.03960	0.04783	0.02142	0.46379
NO3-	0.93197	0.01385	0.05223	0.01662	0.04249	0.06261	0.05483	0.04642	0.02919
SO42-	0.02345	0.89791	0.21637	0.07557	0.25400	0.36650	0.30689	0.28024	0.17074
NH4+	0.00226	0.00435	0.01291	0.00775	0.01293	0.01700	0.01557	0.02567	0.00891
Sb	0.00011	0.00008	0.00074	0.00031	0.00087	0.00122	0.00121	0.00882	0.00162
As	0.00000	0.00000	0.00006	0.00000	0.00010	0.00013	0.00008	0.00089	0.00020
Al	0.00034	0.00014	0.00087	0.00052	0.00094	0.00094	0.00088	0.01111	0.00307
Br	0.00003	0.00000	0.00001	0.00001	0.00001	0.00002	0.00001	0.00109	0.00001
Ca	0.00014	0.00041	0.00474	0.00083	0.02051	0.00118	0.00868	0.00106	0.00110
Cr	0.00008	0.00006	0.00064	0.00023	0.00081	0.00132	0.00123	0.00865	0.00174
Cu	0.00000	0.00000	0.00004	0.00001	0.00002	0.00012	0.00001	0.00103	0.00005
Cl	0.00000	0.00001	0.00003	0.00001	0.00004	0.00704	0.00003	0.00005	0.00002
Fe	0.00087	0.00094	0.00771	0.00189	0.01243	0.00510	0.05442	0.00455	0.00544
Pb	0.00000	0.00000	0.00001	0.00000	0.00002	0.00011	0.00001	0.00102	0.00001
Mn	0.00000	0.00000	0.00001	0.00001	0.00001	0.00005	0.00001	0.00089	0.00001
Mg	0.00018	0.00017	0.00126	0.00051	0.00155	0.00150	0.00138	0.01066	0.00175
Se	0.00000	0.00000	0.00007	0.00000	0.00009	0.00014	0.00009	0.00089	0.00020
Ti	0.00001	0.00000	0.00004	0.00001	0.00002	0.00015	0.00001	0.00097	0.00015
V	0.00000	0.00000	0.00006	0.00000	0.00009	0.00013	0.00008	0.00088	0.00023
Si	0.00019	0.00027	0.00130	0.00044	0.05397	0.00107	0.00108	0.00088	0.00054
Zn	0.00000	0.00000	0.00001	0.00001	0.00001	0.00003	0.00001	0.00040	0.00001
Sr	0.00000	0.00000	0.00010	0.00000	0.00006	0.00014	0.00005	0.00088	0.00024
Tb	0.00000	0.00000	0.00004	0.00000	0.00010	0.00015	0.00009	0.00088	0.00018
Rb	0.00000	0.00000	0.00007	0.00000	0.00008	0.00014	0.00009	0.00087	0.00022
K	0.00003	0.00037	0.04200	0.00003	0.00227	0.00010	0.00011	0.00007	0.00005
Na	0.00087	0.00082	0.00548	0.00290	0.00522	0.00841	0.00597	0.03985	0.00628
Zr	0.00000	0.00000	0.00007	0.00000	0.00007	0.00015	0.00008	0.00089	0.00021

Table 4. Posterior mean of the Λ matrix estimated from all three sites.

	Sec. Nit.	Sec. Sulf.	Biomass	Mobile	Soil	Road Salt	Industry	Bromine	Diesel
OC	0.02446	0.06258	0.53628	0.89619	0.47868	0.50227	0.57831	0.54184	0.33642
EC	0.00442	0.00568	0.03715	0.00964	0.01490	0.02426	0.03283	0.02614	0.46634
NO3-	0.94837	0.01400	0.05484	0.01597	0.04602	0.05324	0.04525	0.05446	0.02625
SO42-	0.01872	0.91105	0.29372	0.06496	0.33254	0.37350	0.23289	0.32815	0.14593
NH4+	0.00189	0.00398	0.01287	0.00687	0.02327	0.01617	0.01343	0.01752	0.00838
Sb	0.00007	0.00004	0.00081	0.00027	0.00772	0.00181	0.00137	0.00246	0.00090
As	0.00000	0.00000	0.00007	0.00000	0.00077	0.00017	0.00012	0.00027	0.00011
Al	0.00024	0.00012	0.00125	0.00037	0.00971	0.00249	0.00098	0.00291	0.00134
Br	0.00001	0.00000	0.00003	0.00001	0.00082	0.00016	0.00004	0.00032	0.00001
Ca	0.00009	0.00085	0.00544	0.00086	0.00091	0.00119	0.02345	0.00129	0.00101
Cr	0.00004	0.00004	0.00068	0.00022	0.00744	0.00179	0.00145	0.00236	0.00121
Cu	0.00000	0.00000	0.00001	0.00000	0.00101	0.00001	0.00000	0.00001	0.00000
Cl	0.00000	0.00000	0.00002	0.00001	0.00003	0.00436	0.00002	0.00002	0.00001
Fe	0.00075	0.00080	0.00554	0.00152	0.00410	0.00485	0.05957	0.00486	0.00532
Pb	0.00000	0.00000	0.00001	0.00000	0.00100	0.00010	0.00001	0.00002	0.00001
Mn	0.00000	0.00001	0.00001	0.00001	0.00098	0.00004	0.00001	0.00003	0.00001
Mg	0.00011	0.00011	0.00096	0.00042	0.00959	0.00231	0.00256	0.00265	0.00109
Se	0.00000	0.00000	0.00005	0.00000	0.00082	0.00018	0.00013	0.00029	0.00003
Ti	0.00000	0.00000	0.00003	0.00000	0.00090	0.00015	0.00001	0.00023	0.00005
V	0.00000	0.00000	0.00007	0.00000	0.00077	0.00017	0.00013	0.00027	0.00010
Si	0.00013	0.00011	0.00056	0.00031	0.01761	0.00077	0.00046	0.00080	0.00033
Zn	0.00000	0.00000	0.00001	0.00001	0.00043	0.00003	0.00001	0.00004	0.00001
Sr	0.00000	0.00000	0.00005	0.00000	0.00077	0.00017	0.00013	0.00028	0.00012
Tb	0.00000	0.00000	0.00002	0.00000	0.00078	0.00015	0.00014	0.00028	0.00013
Rb	0.00000	0.00000	0.00007	0.00000	0.00077	0.00017	0.00012	0.00026	0.00012
K	0.00000	0.00001	0.04375	0.00001	0.00002	0.00002	0.00002	0.00002	0.00001
Na	0.00069	0.00062	0.00568	0.00235	0.03684	0.00927	0.00644	0.01194	0.00469
Zr	0.00000	0.00000	0.00006	0.00000	0.00078	0.00018	0.00013	0.00027	0.00008

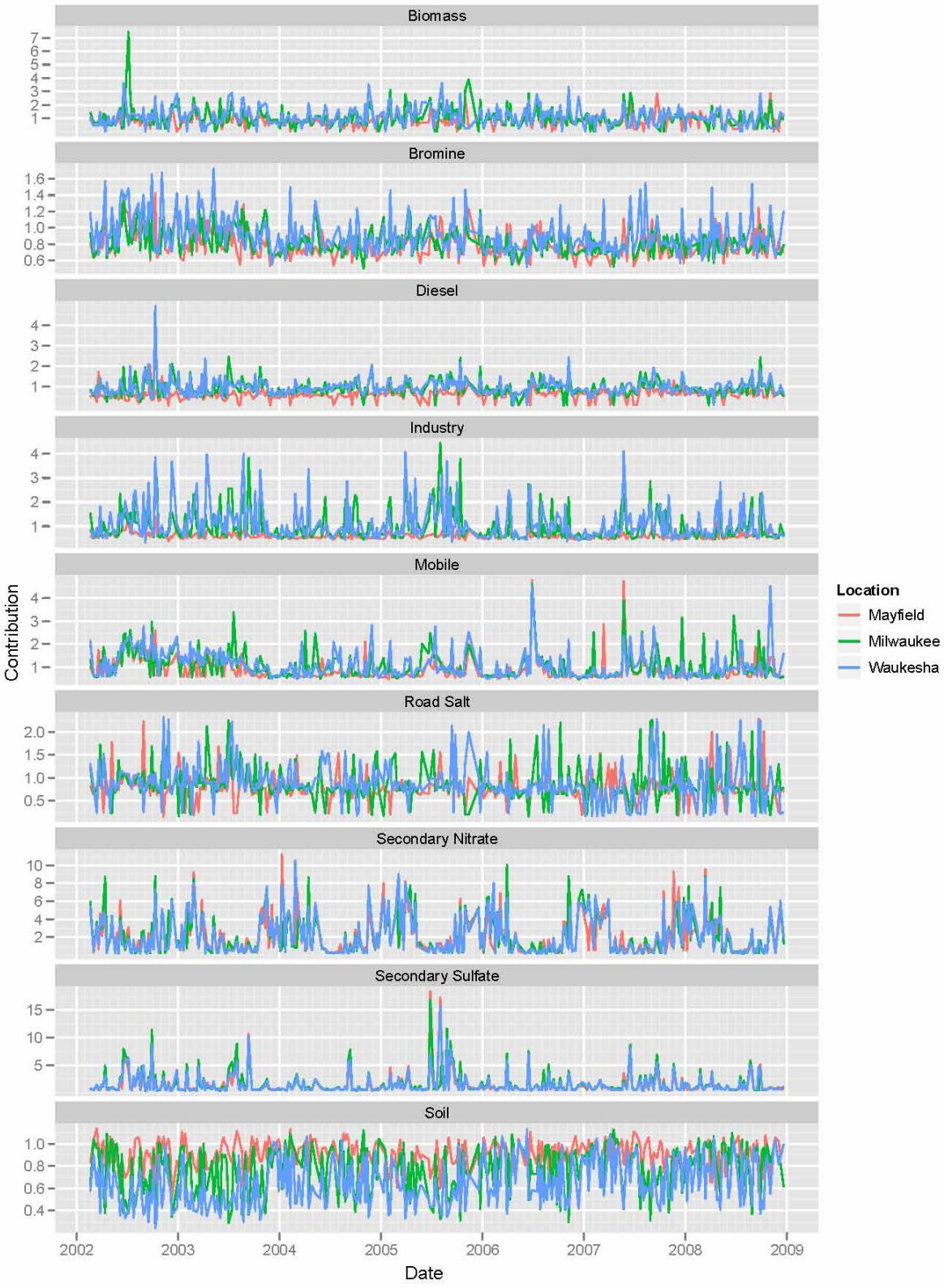

Figure 19: Contribution levels for the three sites as estimated using the common model.

Synoptic Regimes

To determine whether synoptic regimes have an effect on measured pollution concentration levels a Bayesian PSA model was fit following Lingwall, Christensen, and Reese [2008]. Based on previous work, a model was fit using nine sources to predict the concentrations of twenty-eight pollutants measured at the Milwaukee measuring station. The mean posterior distribution for the contribution level is used as a point estimate for the contributions measured for each source on each day. A MANOVA analysis was performed using these point estimates for each of the nine sources as response variables and regime classifications. The MANOVA test and individual ANOVA tests on each source's contributions are highly significant, with all p-values < 0.0001. Plots of the estimated coefficients, showing clear regime effects, are given in Figure 20.

The first two discriminant functions account for over 90% of the total variation in the regime-specific means. The first discriminant function is driven by the contrast between the generic bromine source and the sum of the soil dust and diesel fuel sources. The second discriminant function is primarily a contrast between soil dust and automobile exhaust. Unfortunately, neither of these discriminant functions offers obvious insight into the behavior of the sources.

A plot of the mean discriminant scores for each of the regimes is given in Figure 21. Note the clustering of regimes 1, 3, and 8, and the distance of regime 5, in particular, from the others.

While synoptic regimes do have an effect on measured pollution data, none of the estimates have credible intervals extending below approximately 0.4 μg/m3. This may be the result of a real lack of a complete masking effect or may be an effect of the models, as the log normal prior on the elements of F will tend to pull low estimates away from zero. This analysis clearly indicates that regime data can help estimate contribution levels.

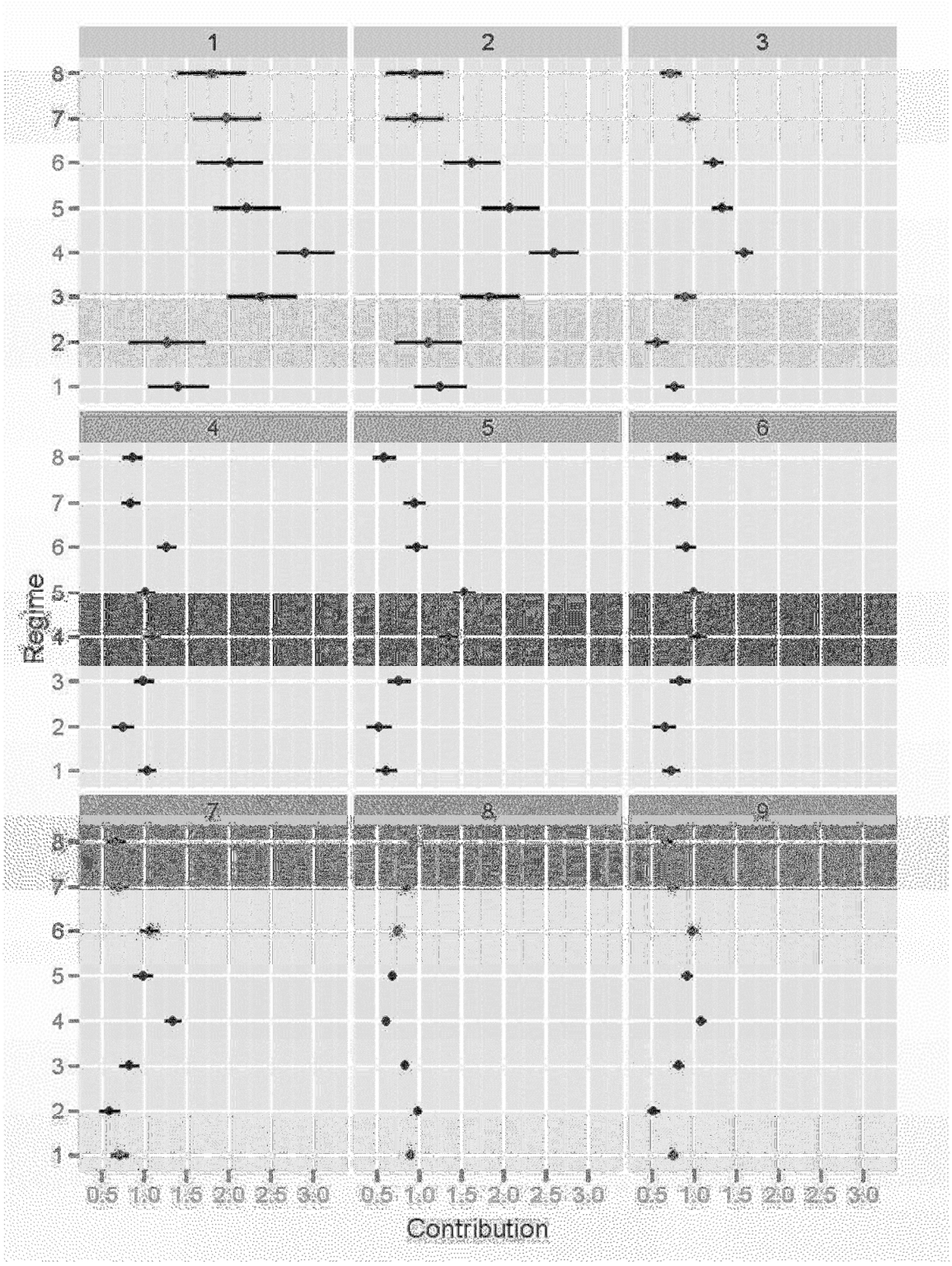

Figure 20. Estimated regime effects (point estimates and 95% confidence intervals) for each of the nine sources.

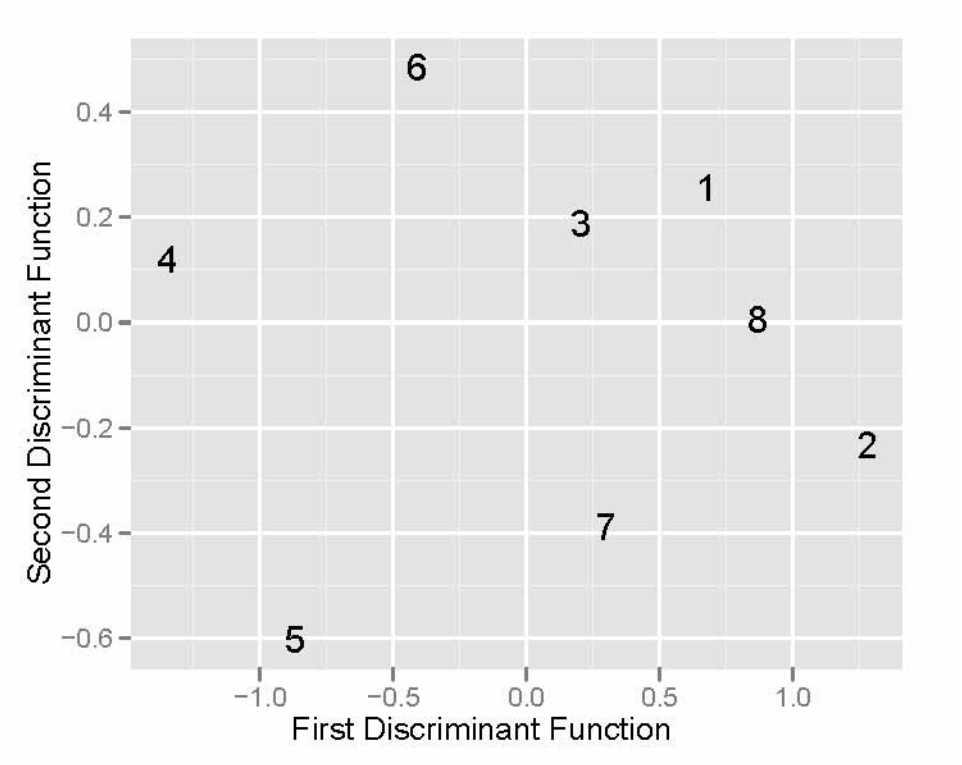

Figure 21. Mean discriminant scores of the eight regimes for the first two discriminant functions.

We attempt to capitalize on this knowledge by fitting the model

$$Y = \Lambda\,[F \circ (MR)] + E$$

This parameterization differs slightly from that originally proposed in that rather than zeroing F out entirely when the source is masked it is replaced with the log normal distribution which will pull estimates away from zero, while an exponential distribution will push estimates toward zero. This approach retains the ability to estimate the masking matrix while allowing regimes to only partially mask a source. The exponential distribution is chosen to cross with the previously chosen log normal prior at an arbitrary point (in this case, 1/3 μg/m3), and may vary from element to element if informative priors on the contributions matrix are used. Thus, if the estimated contribution level for a given source on a given day is below 1/3 μg/m3, the estimate will be pushed toward zero and the model will favor masking that source under the regime to which that day belongs; otherwise, the estimate will be pulled away from zero and the model will not favor masking the source. This approach has been influenced in part by Val Johnson's work on non-local priors [2010]. Unfortunately, in practice we have been unable to fit this model (or

the slightly simpler one originally proposed) and obtain anything resembling MCMC convergence with either real or artificial datasets. The various difficulties encountered are a subject of continuing contemplation though not active research.

Summary of Findings

Milwaukee and Waukesha Counties are currently designated as nonattainment of USEPA air quality standards for fine particulate matter. The Milwaukee, Mayville and Waukesha, WI STN data from 2002-2008 has been analyzed using a number of statistical methods including the US EPA's Positive Matrix Factorization (PMF) analysis to look for trends in concentrations and sources, as well as the urban excess pollution in Milwaukee and Waukesha compared to Mayville. The STN data analysis results show similar yearly trends for chemical composition across all sites. The data also shows an excess of organic matter and elemental carbon in the urban areas of Milwaukee and Waukesha compared to Mayville, and an excess of metals in Waukesha compared to Milwaukee and Mayville. The PMF shows secondary sulfate and secondary nitrate make up over half of the PM 2.5 and there is no urban excess of these sources; however, there is an urban excess of industrial sources in Milwaukee and Waukesha compared to Mayville. Time series plots of the concentrations show many of the concentrations of various elements decreasing while the concentration of chlorine and bromine are increasing significantly. Based on all of the findings it appears regional controls as well as local restrictions would be necessary to decrease the PM 2.5 concentration in Milwaukee and Waukesha Counties to bring them into attainment.

Extreme events or episodes of ambient fine particulate matter (PM2.5), in which daily mass concentrations are substantially higher than annual averages, have been frequently observed in southern Wisconsin. Determining the nature of the events has been a great challenge for the local governments responsible for protecting public health and complying with the 24-hour PM2.5 standard. This study analyzed the air parcels movements that originate in emission source areas and the trends in PM2.5 concentrations in order to determine the important factors involved in elevated regional PM2.5 episodes. Single backward trajectory analysis coupled with PM2.5 concentrations, observed at the Federal Reference Method Network (FRM) site in Madison, Milwaukee and Waukesha along with nitrate and sulfate concentrations, monitored at the Chemical Speciation Network (CSN) site in Milwaukee, Wisconsin, from 2002 to 2010 were

examined. The PM2.5 concentrations from FRM showed total PM2.5 mass during the episodes were higher in Madison than in Milwaukee and Waukesha while annual average concentrations were lower in Madison. However, the temporal trend in the frequency of the elevated PM2.5 episodes occurrence was remarkably similar across the sites during the entire study period, with high PM2.5 episodes occurring from 2005 to 2007. Residence time analysis of backward trajectories calculated for all recorded data indicated episode changes were mainly driven by year-to-year variations of the movements of air masses that originated in high emissions areas. Furthermore, the results of the Potential Source Contribution Function (PSCF) showed that the extreme events of PM2.5 occurred in the region when trajectories endpoints were predominantly located in areas of large ammonia and stationary emissions. The enhanced nitrate and sulfate concentrations which were the major components during the episodes, were strongly influenced by the air masses originating in the Ohio River Valley and adjacent states where large stationary emission sources are located.

A summer intensive study was performed in Milwaukee, Wisconsin in July and August 2010 to identify potential sources of nickel, vanadium and black carbon in the atmosphere. An Aerosol Time-of-Flight Mass Spectrometer (ATOFMS) was used to collect single-particle mass spectra and an aethalometer was used to measure black carbon. A comparison with the National Emissions Inventory was performed using mesoscale meteorological simulations based on the Weather Research and Forecasting model (WRF) and the Comprehensive Air-quality Model with eXtensions (CAMx). The analysis suggests nickel and vanadium are primarily emitted by industrial point sources in the Menomonee valley and black carbon is primarily associated with mobile sources and emissions of nitrogen oxides. Evaluation of ship emissions from the port of Milwaukee suggest these are responsible for less than 5% of nickel and vanadium and less than 10% of black carbon in Milwaukee. Elevated concentrations of air pollutants were found to occur mainly during wind stagnation events suggesting local sources dominate over regional transport.

References

Ashbaugh, L. L., W. C. Malm, and W. Z. Sadeh (1985), A residence time probability analysis of sulfur concentrations at Grand Canyon National Park, *Atmospheric Environment (1967)*, *19*(8), 1263–1270.

Baek, J., Carmichael, G., Lee, S., Oleson, J., Riemer, N., Rohlf, T., Sousan S., Spak, S., Stainer, C. (2010). Episodic air pollution in Wisconsin (LADCO Winter Nitrate Study) and Georgia (SEARCH Network) during Jan-Mar 2009.

De Foy, B. et al. (2007), Modelling constraints on the emission inventory and on vertical dispersion for CO and SO2 in the Mexico City Metropolitan Area using Solar FTIR and zenith sky UV spectroscopy, *Atmospheric Chemistry and Physics*, *7*(3), 781–801.

Draxler, R.R. and Rolph, G.D., (2012). HYSPLIT (Hybrid Single-Particle Lagrangian Integrated Trajectory) Model access via NOAA ARL READY Website (http://ready.arl.noaa.gov/HYSPLIT.php). NOAA Air Resource Laboratory, Silver Spring, MD.

ENVIRON (2011), CAMx, User's guide, Comprehensive Air Quality Model with eXtensions, Version 5.40. ENVIRON International Corporation.

Gertler, A. W., J. A. Gillies, W. R. Pierson, C. F. Rogers, J. C. Sagebiel, M. Abu-Allaban, W. Coulombe, L. Tarnay, and T. A. Cahill (2002), Real-world particulate matter and gaseous emissions from motor vehicles in a highway tunnel, *Res Rep Health Eff Inst*, (107), 5–56; discussion 79–92.

Johnson, V. E., and D. Rossell (2010), On the use of non-local prior densities in Bayesian hypothesis tests, *Journal of the Royal Statistical Society: Series B (Statistical Methodology)*, *72*(2), 143–170.

Katzman, T.L., Rutter, A.P., Schauer, J.J., Lough, G.C., Kolb, C.J., Van Klooster, S. (2010). PM2. 5 and PM10-2.5 Compositions during Wintertime Episodes of Elevated PM Concentrations across the Midwestern USA. Aerosol and Air Quality Research 10, 140–153.

Kim, E., and P. K. Hopke (2004), Improving source identification of fine particles in a rural northeastern US area utilizing temperature-resolved carbon fractions, *Journal of geophysical research*, *109*(D9), D09204.

LADCO (2009), Lake Michigan Air Directors Consortium, Conceptual model of PM2.5 episodes in the Midwest.

Lee, J. H., and P. K. Hopke (2006), Apportioning sources of PM2. 5 in St. Louis, MO using speciation trends network data, *Atmospheric Environment*, *40*, 360–377.

Lingwall, J. W., W. F. Christensen, and C. S. Reese (2008), Dirichlet based Bayesian multivariate receptor modeling, *Environmetrics*, *19*(6), 618–629, doi:10.1002/env.902.

Paatero, P., and U. Tapper (1994), Positive matrix factorization: A non-negative factor model with optimal utilization of error estimates of data values, *Environmetrics*, *5*(2), 111–126.

Polissar, A. V., P. K. Hopke, P. Paatero, W. C. Malm, and J. F. Sisler (1998), Atmospheric aerosol over Alaska 2. Elemental composition and sources, *Journal of Geophysical Research. D. Atmospheres*, *103*, 19–045.

Polissar, A. V., P. K. Hopke, and R. L. Poirot (2001), Atmospheric aerosol over Vermont: chemical composition and sources, *Environmental science & technology*, *35*(23), 4604–4621.

Pope, C.A., Dockery, D. (2006). Health effects of fine particulate air pollution: lines that connect. Journal of the Air & Waste Management Association 56, 709–742.

Pope, C.A., Ezzati, M., Dockery, D.W. (2009). Fine-particulate air pollution and life expectancy in the United States. New England Journal of Medicine 360, 376–386.

Seinfeld, J.H., and Pandis, S. N. (1998). Atmospheric chemistry and physics, from air pollution to climate change. John Wiley and Sons, Inc.

Skamarock, W. C., J. B. Klemp, J. Dudhia, D. O. Gill, D. M. Barker, W. Wang, and J. G. Powers, (2005), A description of the Advanced Research WRF Version2NCAR/TN-468+STR.

Stohl, A., C. Forster, A. Frank, P. Seibert, and G. Wotawa (2005), Technical note: The Lagrangian particle dispersion model FLEXPART version 6.2, *Atmos. Chem. Phys.*, *5*(9), 2461–2474, doi:10.5194/acp-5-2461-2005.

Zhao, W., and P. K. Hopke (2006), Source investigation for ambient PM 2.5 in Indianapolis, IN, *Aerosol science and technology*, *40*(10), 898–909.